Identification and characterization of suppressors of the non-fermentable carbon source defects of *coa1Δ*

by

Yunfeng Zhao

A dissertation submitted to the Graduate Faculty of Auburn University in partial fulfillment of the requirements for the Degree of Doctor of Philosophy

Auburn, Alabama
December 14, 2013

Keywords: *ATP synthase*, cytochrome c oxidase, *Saccharomyces cerevisiae.*

Approved by

Paul A. Cobine, Chair, Assistant Professor of Biological Sciences
Mark R. Liles, Associate Professor of Biological Sciences
Aaron M Rashotte, Assistant Professor of Biological Sciences
Joanna Wysocka-Diller, Associate Professor of Biological Sciences

Abstract

The assembly of cytochrome c oxidase (COX) in yeast mitochondria is dependent on the assembly factor Coa1. *ATP1* was identified as a multi-copy suppressor of the *coa1*Δ respiration defect. *ATP1* is additive with previously discovered suppressors, *MSS51, COX10, MDJ1*, suggesting *ATP1* functions via a different pathway. Using biochemical and microscopic approaches we found *ATP1* rescues a previously unrecognized mitochondrial biogenesis defect in *coa1*Δ that result in low total mitochondrial numbers and a morphology defect. *ATP1* overexpression did not rescue the closely related assembly factor mutant *shy1*Δ. Mitochondrial morphology and biogenesis is dependent on intact mitochondrial ultrastructure. *ATP1* and *COA1* were found to rescue a defect in *aim37*Δ*,* a member of the mitochondrial inner membrane organization and structure (MINOS) complex. We propose the rescue of respiration in *coa1*Δ by multi-copy *ATP1* is due to increased mitochondrial biogenesis perhaps due to improved inner membrane organization in *coa1*Δ or improved localization of COX to cristae. We undertook an approach to isolate evolved homozygous diploid strains capable of growth on non-fermentable carbon source in the absence of coa1. To identify the mutations, we used the next generation sequencing. Four haploid strains were sequenced separately and compared to a reference sequence. An optimized sequencing library preparation procedure resulted in 4.1G data for the four strains. The whole genome was covered (99.9%) and with an average coverage of 92. We identified expected and unexpected single nucleotide polymorphisms present in haploid strains. The mechanism of suppression of the *coa1*Δ yeast appears to be linked to a unique

mutation in *COX1* in the mitochondrial genome. To understand intracellular iron handling, we attempted to use a genetic strategy exploiting the hydroxyurea sensitivity of an iron deficiency (*aft1⊿aft2⊿*). We isolated 6 suppressor mutants of *aft1⊿aft2⊿* double mutant that can tolerate HU and attempted to characterize the suppressing mutation. Our result showed that *SPT3* mutation affected total cellular metals and hydroxyurea sensitivity in this background.

Acknowledgments

I'd like to thank Dr. Paul A. Cobine for the opportunity to conduct research under his guidance. I really appreciate his constant support and patience during my research and dissertation work. I also want to thank my advisory committee, Dr. Mark R. Liles, Dr. Aaron M. Rashotte, and Dr. Joanna Wysocka-Diller for always being available and willing to provide advice and support when requested. I want to thank Dr. Stuart B. Price for serving as University Reader. I would also like to thank my colleagues in Dr. Cobine's lab for their encouragement, help and friendship. Finally, I want to express my gratitude to my parents and those who help me out in my difficult times.

Table of Contents

List of Tables

Chapter 3

List of Figures

Chapter 2

Chapter 3

Chapter 4

Chapter 1

Literature review

Mitochondrial structure and function

Mitochondrion is a two membrane organelle that exists in most eukaryotic cells. Mitochondria are the cellular power plants that produce adenosine triphosphate (ATP) for organisms [1]. Mitochondria can vary greatly in both size (0.5 micrometers - 10 micrometers) and number (1 - over 1000) per cell [2] [3], depending on physiological state, organism and tissue type. Although most of a cell's DNA is contained in the cell nucleus, the mitochondrion has its own independent genome. Mitochondrial proteins vary depending on species and the tissue. For example, there are 615 distinct types of proteins identified from human cardiac mitochondria [4], whereas 940 proteins in mouse [5]. The mitochondrial proteome is thought to be dynamically regulated [6]. The mitochondrial outer and inner membranes have different properties. Based on this double membrane characteristic, there are five distinct parts to a mitochondrion, including the outer membrane, the intermembrane space, the inner membrane, and the cristae and matrix. These different compartments carry out specialized functions.

The mitochondrial outer membrane has a similar protein-to-phospholipid ratio to that of the eukaryotic plasma membrane. The mitochondrial outer membrane contains a lot of integral proteins called porins, which can form channels that allow molecules <5 KDa in molecular weight to diffuse from one side of the membrane to the other [2]. For proteins with signaling sequence at

their N-terminus, they can enter the mitochondrion by binding the signaling sequence to a protein called translocase of the outer membrane [7].

The intermembrane space is the space between the outer membrane and the inner membrane. Because small molecules can freely diffuse through the outer membrane, the concentrations of small molecules such as ions and sugars in the intermembrane space are the same as the cytosol [2]. But, the protein composition of this intermembrane space is different from the protein composition of the cytosol [8].

The inner membrane doesn't contain porins, therefore it is highly impermeable to all molecules. Therefore, all ions and molecules need certain transporters to get into the matrix. The translocase of the inner membrane or Oxa1 are responsible for carrying proteins into the matrix [7]. On the inner membrane, the transportation of electron through the electron transport chain creates a membrane potential across them inner membrane which can be used by the ATP synthase to produce ATP. In total, there are five function proteins on the mitochondrial inner membrane: Those that perform the redox reactions of oxidative phosphorylation; ATP synthase, which generates ATP in the matrix; Specific transport proteins that regulate metabolite passage into and out of the matrix; Protein import machinery; Mitochondria fusion and fission protein.

The cristae are formed by infoldings of the inner membrane, which increase the surface area of the inner mitochondrial membrane, for example,

the liver mitochondrial inner membrane has five times area as great as the outer membrane. The ratio varies depending on the demand for ATP.

The matrix inside the inner membrane contains about 2/3 of the total protein in a mitochondrion [2]. It contains a highly concentrated mixture of hundreds of enzymes, which function in the oxidation of pyruvate and fatty acids, and the citric acid cycle [2]. In addition to enzymes, the matrix also contains special mitochondrial ribosomes, tRNA, and several copies of the mitochondrial DNA genome. As for DNA genome, mitochondria have their own genetic material and the machinery to manufacture their own RNAs and proteins. The human mitochondrial DNA encodes 37 total genes, including 22 tRNA, 2 rRNA, and 13 peptide genes [9]. These 13 mitochondrial peptides and proteins encoded by nuclear genes are both integrated into the inner mitochondrial membrane. The matrix plays an important role in the production of ATP by ATP synthase.

A major function of the mitochondria is to produce ATP and regulate cellular metabolism [3]. There are a large number of proteins in the inner membrane responsible for this function. This task is done by oxidizing the major products of glucose, pyruvate, and NADH, which are produced in the cytosol [3]. This aerobic respiration process is dependent on the presence of oxygen. When oxygen is limited, the glycolytic products will be metabolized by anaerobic fermentation. The anaerobic fermentation process is independent of the mitochondria [3]. The aerobic respiration can produce 13 times amount of

ATP from glucose compared to fermentation [10]. After glycolysis, the produced pyruvate molecule is transported into the matrix, and then oxidized and combined with coenzyme A to form CO_2, acetyl-CoA, and NADH [3]. The acetyl-CoA enters the citric acid cycle as substrate. Except for the succinate dehydrogenase, most enzymes involved in the citric acid cycle are in the mitochondrial matrix. As part of Complex II, the succinate dehydrogenase is located on the inner mitochondrial membrane [11]. During the citric cycle, the acetyl-CoA is oxidized to carbon dioxide. Additionally, three molecules of NADH, one molecule of FADH2 and one molecule of GTP are produced during the citric cycle. The GTP will be converted to an ATP [3]. The reduced cofactors NADH and FADH2 provide electrons for the electron transport chain. These energy-rich molecules are not only produced within the matrix, but are also produced in the cytoplasm by glycolysis. Those energy-rich molecules produced in the cytoplasm are imported by the malate-aspartate shuttle system of antiporter proteins or feed into the electron transport chain via a glycerol phosphate shuttle [3]. During the electron transportation, the electron transport chain complex I, III, IV (cytochrome c oxidase) in the inner membrane pump protons into the intermembrane space, and therefore a strong electrochemical gradient is established across the inner membrane. The proton gradient can be used by the ATP synthase to produce ATP from ADP and inorganic phosphate [3]. During this process, the protons in the intermembrane space return to the matrix through ATP synthase. Under

certain conditions, protons can re-enter the mitochondrial matrix without contributing to ATP synthesis. This process is called proton leak, during which the potential energy of the proton electrochemical gradient is released as heat [3].

Besides energy providing, mitochondria has its function in many other physiological and biochemical mechanisms, such as signaling, regulation of the membrane potential [3] regulation of cellular metabolism [12], the control of the cell cycle and cell growth, cellular differentiation, cell death [12]. Mitochondria deficiency can cause many human diseases, including mitochondrial disorders [13] and cardiac dysfunction [14], and was suggested affecting aging process.

Mitochondrial genome, replication and inheritance

The mitochondria genome has a very high proportion of coding DNA and an absence of repeats. Mitochondrial genes are transcribed as polycistronic transcripts, and then be cleaved and polyadenylated to finally get mature mRNAs. Most proteins necessary for mitochondrial function are coded by nuclear genes, rather than the mitochondrial genome. These nuclear gene encoded proteins are imported into the mitochondrion [9].

Animal mitochondrial genome is usually a single circular chromosome and about 16 kb long. There are 37 genes encoded, which is highly conserved, but may vary in location. The 37 genes in human mitochondrial genome include 13

genes encoding ETC complexes I, III, IV and V subunits, 22 genes encoding mitochondrial tRNA, and 2 genes encoding rRNA [15]. There can be two to ten copies of mitochondrial genomes in one mitochondrion [16]. Although most mitochondria genomes are circular, there are exceptions. Although most mitochondria don't have introns, like the human mitochondrial genome [9], there are some species, such as yeast [17] and protists [18], have introns observed.

In the past, it was thought that mitochondria divide by binary fission similar to bacterial cell division. Now, it is known that mitochondria actually divide by budding. There are some differences about this division between eukaryotes. In some eukaryotes, the mitochondrial DNA replication and division mainly according to the energy needs of the cell. If a cell needs more energy, mitochondria will grow and divide. On the contrary, if the cells do not need that much energy, mitochondria are destroyed or become inactive. In this case, mitochondria are randomly distributed to the daughter cells during the division of the cytoplasm. But, in many single-celled eukaryotes, the mitochondrial growth and division is related to the cell cycle. For example, a single mitochondrion may divide synchronously with the nucleus. This division and segregation process must be tightly regulated so that each daughter cell receives at least one mitochondrion. In addition to fission, mitochondria can fuse with other mitochondria [15][19]. The change between mitochondrial

fusion and fission affects mitochondrial function and often associate with disease conditions [20].

ATP synthesis and the regulation of electron transport chain

The biogenesis of ATP can be produce by glycolysis or through oxidative phosphorylation (OXPHOS) and electron transport chain (ETC). The ETC are composed of five protein complexes and two mobile electron carriers. The electrons come from OXPHOS are transported through the ETC and the transportation help protons to be pumped from the mitochondria matrix into the intermembrane space to generate a proton gradient across the inner membrane. This proton gradient can be used by complex V to synthesize ATP. In yeast *Saccharomyces cerevisiae,* ATP synthesis is regulated by carbon source and oxygen concentration, whereas in the mammalian cells this process is mainly affected by the oxygen concentration, muscle contraction and hormone [21] [22] [23] [24]. About the regulation of the ETC, there are two models. One model proposed that the mitochondrial respiration is stimulated by the decrease of proton gradient along with the ATP synthesis [25] [26]. The other model proposed that the phosphorylation state of COX is the key regulation point. This latter model is supported by the finding that COX is inhibited at high ATP-ADP ratio in the mitochondria [27]. This regulation is short term and immediate because it works through a change of enzyme kinetics and doesn't require protein synthesis and assembly. There is also a

long term regulation of COX that works through controlling the COX molecule number or changing the subunit isoform composition of the enzymes. In this review, we will talk about COX assembly process and its regulation at different levels with *S. cerevisiae* model.

The structure, assembly and regulation of COX

In yeast ETC is required for growth on non-fermentable carbon sources. Cytochrome c oxidase (COX) is the terminal enzyme of the electron transport chain (ETC). The assembly of COX needs subunits and assembly factors encoded in nuclear genome and mitochondrial genome. The biosynthesis of the holoenzyme includes the coordinated synthesis of mitochondrial-encoded subunits and nuclear-encoded subunits, the importation of the nuclear-encoded subunits into mitochondria, the insertion of all the nuclear-encoded and mitochondrial-encoded structural subunits into the mitochondrial inner membrane, insertion of the cofactors, assembly of all the structural subunits, dimerization and formation of supercomplexes.

COX from *S. cerevisiae* consists of 11 structural subunits. The three largest subunits, Cox1, Cox2, and Cox3, form the catalytic core of the enzyme and are mitochondrial encoded. The cofactors including heme A and copper ions are inserted into these core subunits. There are two redox centers in the Cox1 subunit. One formed by heme A and the other formed by heme a_3 and Cu_B. Two copper ions form the third redox center at Cu_A site of Cox2. The

electron carried on cytochrome c was transferred in the order: Cu_A site, heme A, and heme a_3-Cu_B site where molecular oxygen was reduced to H_2O [28].

The other smaller nuclear-encoded subunits around the catalytic core are transcribed and translated in the cytoplasm and then imported into mitochondria. The functions of these subunits are not completely clarified yet. They are not essential for reducing oxygen and pumping proton, but the research about yeast strains carrying null mutations in nuclear genes encoding for subunits Cox4, Cox5, Cox6, Cox7, and Cox9 showed that these nuclear-encoded subunits play an essential role in the assembly, stability and dimerization of the enzyme [29] [30] [31] [32] [33].

The assembly of the nuclear-encoded subunits and the mitochondrial-encoded ones is a highly regulated process, which include two different pathways of transcription, translation, maturation and mitochondrial importation. The COX assembly also requires a lot of assembly factors at different level. Research about respiratory deficient mutants found there are more than 20 nuclear genes encoding assembly factors [38] [39]. They participate in all the processes of COX assembly [40] [41] [42].

S. cerevisiae growing in medium containing glucose, will perform glycolysis and fermentation. Under this growth condition, the genes encoding proteins for respiratory growth are repressed. After the glucose is exhausted, yeast will switch to respiratory growth provided oxygen is available. The change from fermentation to respiratory growth is called diauxic shift. During

the diauxic shift, the COX activity increases five fold [43] [44][24]. The COX activity change during the diauxic shift is modulated by the regulation of COX biogenesis. And the COX biogenesis is mainly regulated by the expression of its structural subunits and assembly factors.

Transcription of mitochondrial genes for COX assembly

The expression of mitochondrial encoded COX subunits, like the three core subunits, is also regulated by oxygen and carbon source. The *COX1* mRNA is almost at the same level under different oxygen concentrations, but the *COX3* mRNA level decrease twofold to threefold under anaerobic condition. Although the mitochondrial COX genes are also repressed by glucose and induced during the diauxic shift [69] [70], after being released from glucose repression, the final change in RNA level are quite different between RNA species [70].

Hap complex probably also involved in the expression of mitochondrial DNA genes, because overexpression of Hap4 results in an increase of both *COX1* and *COX2* mRNA level in repressed cells [68].

Translation of mitochondrial genes for COX assembly

The expression of nuclear-encoded COX subunits is mainly regulated at the transcriptional level. But for the expression of mitochondria encoded subunits, there are many translational activators involved. Pet309 and Mss51

involve in the translation of *COX1* mRNA [75] [76]. Pet111 involves in the translation of *COX2* mRNA [77]. Pet54, Pet494 and Pet122 involve in the translation of *COX3* mRNA [78] [79]. These translation activators are inner membrane proteins that can help to couple the mitochondrial translation with the inner membrane. This characteristic allows the cotranslational insertion of newly synthesized subunits into the membrane [80]. Except for translational activator Mss51, other translational activators were found to interact with each other [80] [81]. The interactions of these translation activators are not necessary for them to retain their activity, because they still can retain their activity when some is absent. But overexpressing the *COX2* translational activator Pet111 can repress the translation of *COX1* mRNA, which suggests the amount of different activators is probably important [82].

The function of *MSS51* and *PET309* in *COX1* expression is to help mature and translate *COX1* mRNA [75] [76]. The mutant forms of mss51 or overexpression of the wild type gene can increase the expression of Cox1, and this mechanism can be used to suppress the deficiency of *SHY1*-null mutants [83]. The Shy1 involves in the maturation and assembly of Cox1p [83] [84] [85]. The newly synthesized Cox1 is not only decreased in shy1-null mutants, but also in most COX assembly mutants. These deficiencies can be suppressed by *MSS51* suppressor of *shy1*Δ or by mutations in *COX14*. Mss51 is not only involved in acting on the 5'-UTR to initiate translation like other translation activators did, but also involved in translation elongation of Cox1 [84]. After the

translation of Cox1, Mss51 and Cox1 will form a transient complex [86] [84]. Then the Cox14 will interact with Cox1 and stabilize the transient complex formed by Mss51 and Cox1. The formation of this ternary complex will down regulate the Cox1 synthesis because of the titration of Mss51 [86]. Later the Mss51 can be released to the Cox1 synthesis process, probably because the help of Shy1 [83]. The translation of *COX2* mRNA is initiated and also limited by its translation activator Pet111, because the concentration of this translation activator is low [77] [87] [88].

Cofactors for COX

Copper and heme A are two cofactors essential for COX assembly and activity. There are three copper atoms in COX. Two copper atoms form the Cu_A site located in Cox2 and the third one is at the Cu_B site in Cox1. In yeast, there are at least five proteins related to the copper delivery and insertion. Three of these proteins, Cox17, Cox19, and Cox23, work for the copper delivery. The Cox17 was thought to be involved in copper homeostasis because the respiratory deficiency of *COX17*-null mutant strains can be rescued by supplementation of copper to the medium [89]. Additionally, Cox17 localizes in both the cytoplasm and the mitochondrial intermembrane space, a way that would facilitate shuttling copper from cytoplasm to intermembrane space [89] [90]. But there are also two problems with Cox17 working as a chaperone for copper delivery. One problem is the complex size formed by

several Cox17 and copper is too big to pass the outer membrane protein channel [91]. The other problem is tethering of Cox17 to the inner mitochondrial membrane doesn't affect COX assembly [92]. The cellular distributions of Cox19 and Cox23 are similar to Cox17 [93] [94]. Beside this three protein chaperones, there are two other chaperones, Cox11 and Sco1, that receive copper from Cox17 and insert copper into COX Cu_A and Cu_B sites [95].

Heme a exists exclusively in COX. The biosynthesis process of heme A includes conversion of heme b in heme O and oxidation of heme O in heme A. The heme A amount in different yeast COX mutants has a great decrease, except for *shy1*-, *cox20*-, and *cox5a*-null mutant. These three mutants still have 10-25% of normal heme A level, which probably associated with residual assembled COX [96]. The heme A level has a significant increase in COX mutants with overexpression of *COX15*. The COX mutant strains that no Cox1 is synthesized also has that great increase, suggesting the drastic decrease or absence of heme A in COX mutants is not because the absence of Cox1, but a feedback regulation of the heme A synthesis when the COX assembly process is blocked. Except for COX10 null-mutant, the other analyzed COX mutants showed an accumulation of heme O, therefore, heme O is considered as a stable state of heme. In addition to that, the *COX15* null-mutant showed a very low heme O concentration, suggesting Cox15 also participates in the first step of heme A synthesis [96].

In conclusion, the fully assembled COX is essential to ATP production. The assembly process is regulated at both transcription and translation levels of nuclear COX genes and mitochondrial COX genes by different environmental stimuli. In addition to that, the assembly process also includes cofactor insertion to form the catalytic core of the enzyme.

Reference:

[1] N. A. Campbell, B. Williamson, and R. J. Heyden, *Biology: Exploring Life*. Boston: Pearson Prentice Hall, 2006.

[2] B. Alberts, A. Johnson, J. Lewis, M. Raff, K. Roberts, and P. Walter, *Molecular Biology of the Cell*. New York: Garland Publishing Inc., 1994.

[3] D. Voet, J. G. Voet, and C. W. Pratt, *damentals of Biochemistry*, 2nd ed. John Wiley and Sons, Inc., 2006, p. 547.

[4] S. W. Taylor, E. Fahy, B. Zhang, G. M. Glenn, D. E. Warnock, S. Wiley, A. N. Murphy, S. P. Gaucher, R. A. Capaldi, B. W. Gibson, and S. S. Ghosh, “Characterization of the human heart mitochondrial proteome.,” *Nature Biotechnology*, vol. 21, pp. 281–286, 2003.

[5] J. Zhang, X. Li, M. Mueller, Y. Wang, C. Zong, N. Deng, T. M. Vondriska, D. A. Liem, J.-I. Yang, P. Korge, H. Honda, J. N. Weiss, R. Apweiler, and P. Ping, “Systematic characterization of the murine mitochondrial proteome using functionally validated cardiac mitochondria.,” *Proteomics*, vol. 8, pp. 1564–1575, 2008.

[6] J. Zhang, D. A. Liem, M. Mueller, Y. Wang, C. Zong, N. Deng, T. M. Vondriska, P. Korge, O. Drews, W. R. Maclellan, H. Honda, J. N. Weiss, R. Apweiler, and P. Ping, “Altered proteome biology of cardiac mitochondria under stress conditions.,” *Journal of Proteome Research*, vol. 7, pp. 2204–2214, 2008.

[7] J. M. Herrmann and W. Neupert, “Protein transport into mitochondria,” *Current Opinion in Microbiology*, vol. 3, pp. 210–4, 2000.

[8] J. E. Chipuk, L. Bouchier-Hayes, and D. R. Green, “Mitochondrial outer membrane permeabilization during apoptosis: the innocent bystander scenario.,” *Cell Death and Differentiation*, vol. 13, pp. 1396–1402, 2006.

[9] S. Anderson, A. T. Bankier, B. G. Barrell, M. H. De Bruijn, A. R. Coulson, J. Drouin, I. C. Eperon, D. P. Nierlich, B. A. Roe, F. Sanger, P. H. Schreier, A. J. Smith, R. Staden, and I. G. Young, “Sequence and organization of the human mitochondrial genome.,” *Nature*, vol. 290, pp. 457–465, 1981.

[10] P. R. Rich, “The molecular machinery of Keilin’s respiratory chain.,” *Biochemical Society Transactions*, vol. 31, pp. 1095–1105, 2003.

[11] A. King, M. A. Selak, and E. Gottlieb, “Succinate dehydrogenase and fumarate hydratase: linking mitochondrial dysfunction and cancer,” *Oncogene*, vol. 25, pp. 4675–4682, 2006.

[12] H. M. McBride, M. Neuspiel, and S. Wasiak, “Mitochondria: more than just a powerhouse.,” *Current biology : CB*, vol. 16, no. 14, pp. R551–60, Jul. 2006.

[13] A. Gardner and R. Boles, “Is a ‘Mitochondrial Psychiatry’ in the Future? A Review,” *Current Psychiatry Reviews*, vol. 1, no. 3, pp. 255–271, Nov. 2005.

[14] E. J. Lesnefsky, S. Moghaddas, B. Tandler, J. Kerner, and C. L. Hoppel, “Mitochondrial dysfunction in cardiac disease: ischemia--reperfusion, aging, and heart failure.,” *Journal of molecular and cellular cardiology*, vol. 33, no. 6, pp. 1065–89, Jun. 2001.

[15] D. C. Chan, “Mitochondria: dynamic organelles in disease, aging, and development.,” *Cell*, vol. 125, no. 7, pp. 1241–52, Jun. 2006.

[16] R. J. Wiesner, J. C. Rüegg, and I. Morano, “Counting target molecules by exponential polymerase chain reaction: copy number of mitochondrial DNA in rat tissues.,” *Biochemical and biophysical research communications*, vol. 183, no. 2, pp. 553–9, Mar. 1992.

[17] S. K. Hebbar, S. M. Belcher, and P. S. Perlman, “A maturase-encoding group IIA intron of yeast mitochondria self-splices in vitro.,” *Nucleic acids research*, vol. 20, no. 7, pp. 1747–54, Apr. 1992.

[18] M. W. Gray, B. F. Lang, R. Cedergren, G. B. Golding, C. Lemieux, D. Sankoff, M. Turmel, N. Brossard, E. Delage, T. G. Littlejohn, I. Plante, P. Rioux, D. Saint-Louis, Y. Zhu, and G. Burger, “Genome structure and gene content in protist mitochondrial DNAs.,” *Nucleic acids research*, vol. 26, no. 4, pp. 865–78, Feb. 1998.

[19] G. J. Hermann, J. W. Thatcher, J. P. Mills, K. G. Hales, M. T. Fuller, J. Nunnari, and J. M. Shaw, “Mitochondrial fusion in yeast requires the transmembrane GTPase Fzo1p.,” *The Journal of cell biology*, vol. 143, no. 2, pp. 359–73, Oct. 1998.

[20] A. Y. Seo, A.-M. Joseph, D. Dutta, J. C. Y. Hwang, J. P. Aris, and C. Leeuwenburgh, “New insights into the role of mitochondria in aging: mitochondrial dynamics and more.,” *Journal of cell science*, vol. 123, no. Pt 15, pp. 2533–42, Aug. 2010.

[21] T. Kadowaki and Y. Kitagawa, “Hypoxic depression of mitochondrial mRNA levels in HeLa cell.,” *Experimental Cell Research*, vol. 192, pp. 243–247, 1991.

[22] D. A. Hood, R. Zak, and D. Pette, “Chronic stimulation of rat skeletal muscle induces coordinate increases in mitochondrial and nuclear mRNAs of cytochrome-c-oxidase subunits.,” *The Federation of European Biochemical Societies Journal*, vol. 179, pp. 275–280, 1989.

[23] T. M. Pillar and H. J. Seitz, “Thyroid hormone and gene expression in the regulation of mitochondrial respiratory function.,” *European journal of endocrinology European Federation of Endocrine Societies*, vol. 136, pp. 231–239, 1997.

[24] C. Wrutniak-Cabello, F. Casas, and G. Cabello, “Thyroid hormone action in mitochondria.,” *Journal of Molecular Endocrinology*, vol. 26, pp. 67–77, 2001.

[25] P. Mitchell, “Chemiosmotic coupling in oxidative and photosynthetic phosphorylation.,” *Biological Reviews of the Cambridge Philosophical Society*, vol. 41, pp. 445–502, 1966.

[26] P. Mitchell, “Coupling of phosphorylation to electron and hydrogen transfer by a chemi-osmotic type of mechanism,” *Nature*, vol. 191, pp. 144–148, 1961.

[27] K. Follmann, S. Arnold, S. Ferguson-Miller, and B. Kadenbach, “Cytochrome c oxidase from eucaryotes but not from procaryotes is allosterically inhibited by ATP.,” *Biochemistry and molecular biology international*, vol. 45, pp. 1047–1055, 1998.

[28] G. T. Babcock and M. Wikström, “Oxygen activation and the conservation of energy in cell respiration.,” *Nature*, vol. 356, no. 6367, pp. 301–9, Mar. 1992.

[29] R. Aggeler and R. A. Capaldi, “Yeast cytochrome c oxidase subunit VII is essential for assembly of an active enzyme. Cloning, sequencing, and characterization of the nuclear-encoded gene.,” *J. Biol. Chem.*, vol. 265, no. 27, pp. 16389–16393, Sep. 1990.

[30] K. M. Calder and J. E. McEwen, “Deletion of the COX7 gene in Saccharomyces cerevisiae reveals a role for cytochrome c oxidase subunit VII in assembly of remaining subunits.,” *Molecular Microbiology*, vol. 5, pp. 1769–1777, 1991.

[31] W. Dowhan, C. R. Bibus, and G. Schatz, “The cytoplasmically-made subunit IV is necessary for assembly of cytochrome c oxidase in yeast.,” *The EMBO journal*, vol. 4, no. 1, pp. 179–84, Jan. 1985.

[32] C. E. Trueblood and R. O. Poyton, “Differential effectiveness of yeast cytochrome c oxidase subunit genes results from differences in expression not function.,” *Molecular and cellular biology*, vol. 7, no. 10, pp. 3520–6, Oct. 1987.

[33] R. M. Wright, L. K. Dircks, and R. O. Poyton, “Characterization of COX9, the nuclear gene encoding the yeast mitochondrial protein cytochrome c oxidase subunit VIIa. Subunit VIIa lacks a leader peptide and is an essential component of the holoenzyme.,” *The Journal of biological chemistry*, vol. 261, no. 36, pp. 17183–91, Dec. 1986.

[34] T. Tsukihara, H. Aoyama, E. Yamashita, T. Tomizaki, H. Yamaguchi, K. Shinzawa-Itoh, R. Nakashima, R. Yaono, and S. Yoshikawa, “The whole structure of the 13-subunit oxidized cytochrome c oxidase at 2.8 A.,” *Science (New York, N.Y.)*, vol. 272, no. 5265, pp. 1136–44, May 1996.

[35] W. Birchmeier, C. E. Kohler, and G. Schatz, “Interaction of integral and peripheral membrane proteins: affinity labeling of yeast cytochrome oxidase by modified yeast cytochrome c.,” *Proceedings of the National Academy of Sciences of the United States of America*, vol. 73, no. 12, pp. 4334–8, Dec. 1976.

[36] V. M. Darley-Usmar, G. Georgevich, and R. A. Capaldi, “Reaction of thionitrobenzoate-modified yeast cytochrome c with monomeric and dimeric forms of beef heart cytochrome c oxidase.,” *FEBS letters*, vol. 166, no. 1, pp. 131–5, Jan. 1984.

[37] S. J. Lee, E. Yamashita, T. Abe, Y. Fukumoto, T. Tsukihara, K. Shinzawa-Itoh, H. Ueda, and S. Yoshikawa, “Intermonomer interactions in dimer of bovine heart cytochrome c oxidase.,” *Acta Crystallographica Section D Biological Crystallography*, vol. 57, pp. 941–947, 2001.

[38] J. McEwen, C. Ko, B. Kloeckner-Gruissem, and R. Poyton, “Nuclear functions required for cytochrome c oxidase biogenesis in Saccharomyces cerevisiae.,” *Journal of Biological Chemistry*, vol. 256, pp. 5041–5045, 1986.

[39] A. Tzagoloff and C. L. Dieckmann, “PET genes of Saccharomyces cerevisiae.,” *Microbiological reviews*, vol. 54, pp. 211–225, 1990.

[40] A. Barrientos, M. H. Barros, I. Valnot, A. Rötig, P. Rustin, and A. Tzagoloff, “Cytochrome oxidase in health and disease.,” *Biochemical Society Transactions*, vol. 286, pp. 1051–1056, 2002.

[41] J. M. Herrmann and S. Funes, “Biogenesis of cytochrome oxidase-sophisticated assembly lines in the mitochondrial inner membrane.,” *Gene*, vol. 354, pp. 43–52, 2005.

[42] O. Khalimonchuk and G. Rödel, “Biogenesis of cytochrome c oxidase.,” *Mitochondrion*, vol. 5, pp. 363–388, 2005.

[43] H. F. Bunn and R. O. Poyton, “Oxygen sensing and molecular adaptation to hypoxia.,” *Physiological Reviews*, vol. 76, pp. 839–885, 1996.

[44] P. S. Perlman and H. R. Mahler, “Derepression of mitochondria and their enzymes in yeast: regulatory aspects.,” *Archives of biochemistry and biophysics*, vol. 162, no. 1, pp. 248–71, May 1974.

[45] R. O. Poyton and P. V Burke, “Oxygen regulated transcription of cytochrome c and cytochrome c oxidase genes in yeast.,” *Biochimica et biophysica acta*, vol. 1101, no. 2, pp. 252–6, Jul. 1992.

[46] P. V Burke, D. C. Raitt, L. A. Allen, E. A. Kellogg, and R. O. Poyton, “Effects of oxygen concentration on the expression of cytochrome c and cytochrome c oxidase genes in yeast,” *JBiolChem*, vol. 272, pp. 14705–14712, 1997.

[47] P. J. Rogers and P. R. Stewart, “Respiratory Development in Saccharomyces cerevisiae Grown at Controlled Oxygen Tension,” *Journal Of Bacteriology*, vol. 115, pp. 88–97, 1973.

[48] P. S. David and R. O. Poyton, “Effects of a transition from normoxia to anoxia on yeast cytochrome c oxidase and the mitochondrial respiratory chain: implications for hypoxic gene induction.,” *Biochimica et Biophysica Acta*, vol. 1709, pp. 169–180, 2005.

[49] J. Saltzgaber-Müller and G. Schatz, “Heme is necessary for the accumulation and assembly of cytochrome c oxidase subunits in Saccharomyces cerevisiae.,” *The Journal of Biological Chemistry*, vol. 253, pp. 305–310, 1978.

[50] J. D. Trawick, R. M. Wright, and R. O. Poyton, “Transcription of yeast COX6, the gene for cytochrome c oxidase subunit VI, is dependent on

heme and on the HAP2 gene.," *The Journal of Biological Chemistry*, vol. 264, pp. 7005–7008, 1989.

[51] C. E. Trueblood, R. M. Wright, and R. O. Poyton, "Differential regulation of the two genes encoding Saccharomyces cerevisiae cytochrome c oxidase subunit V by heme and the HAP2 and REO1 genes.," *Molecular and cellular biology*, vol. 8, pp. 4537–40, 1988.

[52] T. Biliński, J. Lukaszkiewicz, and A. Sledziewski, "Demonstration of anaerobic catalase synthesis in the cz1 mutant of Saccharomyces cerevisiae.," *Biochemical and biophysical research communications*, vol. 83, no. 3, pp. 1225–33, Aug. 1978.

[53] K. E. Kwast, P. V Burke, B. T. Staahl, and R. O. Poyton, "Oxygen sensing in yeast: Evidence for the involvement of the respiratory chain in regulating the transcription of a subset of hypoxic genes," *Proceedings of the National Academy of Sciences of the United States of America*, vol. 96, pp. 5446–5451, 1999.

[54] R. S. Zitomer and C. V Lowry, "Regulation of gene expression by oxygen in Saccharomyces cerevisiae.," *Microbiological reviews*, vol. 56, pp. 1–11, 1992.

[55] J. Verdière, F. Creusot, L. Guarente, and P. P. Slonimski, "The overproducing CYP1 and the underproducing hap1 mutations are alleles of the same gene which regulates in trans the expression of the structural genes encoding iso-cytochromes c.," *Current Genetics*, vol. 10, pp. 339–342, 1986.

[56] L. Zhang and L. Guarente, "Heme binds to a short sequence that serves a regulatory function in diverse proteins.," *the The European Molecular Biology Organization Journal*, vol. 14, pp. 313–320, 1995.

[57] S. L. Forsburg and L. Guarente, "Identification and characterization of HAP4: a third component of the CCAAT-bound HAP2/HAP3 heteromer.," *Genes & Development*, vol. 3, pp. 1166–1178, 1989.

[58] S. Hahn and L. Guarente, "Yeast HAP2 and HAP3: transcriptional activators in a heteromeric complex.," *Science*, vol. 240, pp. 317–321, 1988.

[59] D. S. Mcnabb, "Assembly of the Hap2p / Hap3p / Hap4p / Hap5p-DNA Complex in Saccharomyces cerevisiae," *Society*, vol. 4, pp. 1829–1839, 2005.

[60] S. Buschlen, J.-M. Amillet, B. Guiard, A. Fournier, C. Marcireau, and M. Bolotin-Fukuhara, “The S. Cerevisiae HAP Complex, a Key Regulator of Mitochondrial Function, Coordinates Nuclear and Mitochondrial Gene Expression,” *Comparative and Functional Genomics*, vol. 4, pp. 37–46, 2003.

[61] J. D. Trawick, N. Kraut, F. R. Simon, and R. O. Poyton, “Regulation of yeast COX6 by the general transcription factor ABF1 and separate HAP2- and heme-responsive elements.,” *Molecular and Cellular Biology*, vol. 12, pp. 2302–2314, 1992.

[62] L. Guarente, B. Lalonde, P. Gifford, and E. Alani, “Distinctly regulated tandem upstream activation sites mediate catabolite repression of the CYC1 gene of S. cerevisiae.,” *Cell*, vol. 36, pp. 503–11, 1984.

[63] C. Dagsgaard, L. E. Taylor, K. M. O’Brien, and R. O. Poyton, “Effects of anoxia and the mitochondrion on expression of aerobic nuclear COX genes in yeast: evidence for a signaling pathway from the mitochondrial genome to the nucleus.,” *The Journal of Biological Chemistry*, vol. 276, pp. 7593–7601, 2001.

[64] J. L. DeRisi, V. R. Iyer, and P. O. Brown, “Exploring the metabolic and genetic control of gene expression on a genomic scale.,” *Science*, vol. 278, pp. 680–686, 1997.

[65] R. M. Wright and R. O. Poyton, “Release of two Saccharomyces cerevisiae cytochrome genes, COX6 and CYC1, from glucose repression requires the SNF1 and SSN6 gene products,” *Molecular and Cellular Biology*, vol. 10, pp. 1297–1300, 1990.

[66] R. M. Wright, B. Rosenzweig, and R. O. Poyton, “Organization and expression of the COX6 genetic locus in Saccharomyces cerevisiae: multiple mRNAs with different 3’ termini are transcribed from COX6 and regulated differentially.,” *Nucleic Acids Research*, vol. 17, pp. 1103–1120, 1989.

[67] W. Gunji, T. Kai, Y. Takahashi, Y. Maki, W. Kurihara, T. Utsugi, F. Fujimori, and Y. Murakami, “Global Analysis of the Regulatory Network Structure of Gene Expression in Saccharomyces cerevisiae,” *DNA Research*, vol. 11, pp. 163–177, 2004.

[68] R. Lascaris, H. J. Bussemaker, A. Boorsma, M. Piper, H. Van Der Spek, L. Grivell, and J. Blom, “Hap4p overexpression in glucose-grown Saccharomyces cerevisiae induces cells to enter a novel metabolic state,” *Genome Biology*, vol. 4, p. R3, 2003.

[69] D. M. Mueller and G. S. Getz, “Transcriptional regulation of the mitochondrial genome of yeast Saccharomyces cerevisiae.,” *The Journal of biological chemistry*, vol. 261, no. 25, pp. 11756–64, Sep. 1986.

[70] T. L. Ulery, S. H. Jang, and J. A. Jaehning, “Glucose repression of yeast mitochondrial transcription: kinetics of derepression and role of nuclear genes.,” *Molecular and cellular biology*, vol. 14, no. 2, pp. 1160–70, Feb. 1994.

[71] J. Min and H. P. Zassenhaus, “A nucleoside triphosphate-regulated, 3’ exonucleolytic mechanism is involved in turnover of yeast mitochondrial RNAs.,” *Journal of bacteriology*, vol. 175, no. 19, pp. 6245–53, Oct. 1993.

[72] T. K. Biswas and G. S. Getz, “Promoter-promoter interactions influencing transcription of the yeast mitochondrial gene, Oli 1, coding for ATPase subunit 9. Cis and trans effects.,” *The Journal of Biological Chemistry*, vol. 263, pp. 4844–4851, 1988.

[73] J. Wettstein-Edwards, B. S. Ticho, N. C. Martin, D. Najarian, and G. S. Getz, “In vitro transcription and promoter strength analysis of five mitochondrial tRNA promoters in yeast.,” *The Journal of Biological Chemistry*, vol. 261, pp. 2905–2911, 1986.

[74] D. M. Mueller and G. S. Getz, “Steady state analysis of mitochondrial RNA after growth of yeast Saccharomyces cerevisiae under catabolite repression and derepression.,” *The Journal of biological chemistry*, vol. 261, no. 25, pp. 11816–22, Sep. 1986.

[75] G. M. Manthey and J. E. McEwen, “The product of the nuclear gene PET309 is required for translation of mature mRNA and stability or production of intron-containing RNAs derived from the mitochondrial COX1 locus of Saccharomyces cerevisiae.,” *The EMBO journal*, vol. 14, no. 16, pp. 4031–43, Aug. 1995.

[76] E. Decoster, M. Simon, D. Hatat, and G. Faye, “The MSS51 gene product is required for the translation of the COX1 mRNA in yeast mitochondria.,” *Molecular & general genetics : MGG*, vol. 224, no. 1, pp. 111–8, Oct. 1990.

[77] C. G. Poutre and T. D. Fox, “PET111, a Saccharomyces cerevisiae nuclear gene required for translation of the mitochondrial mRNA encoding cytochrome c oxidase subunit II.,” *Genetics*, vol. 115, no. 4, pp. 637–47, Apr. 1987.

[78] M. C. Costanzo, E. C. Seaver, and T. D. Fox, “At least two nuclear gene products are specifically required for translation of a single yeast mitochondrial mRNA.,” *The EMBO journal*, vol. 5, no. 13, pp. 3637–41, Dec. 1986.

[79] B. Kloeckener-Gruissem, J. E. McEwen, and R. O. Poyton, “Identification of a third nuclear protein-coding gene required specifically for posttranscriptional expression of the mitochondrial COX3 gene is Saccharomyces cerevisiae.,” *Journal of bacteriology*, vol. 170, no. 3, pp. 1399–402, Mar. 1988.

[80] S. Naithani, S. A. Saracco, C. A. Butler, and T. D. Fox, “Interactions among COX1, COX2, and COX3 mRNA-specific translational activator proteins on the inner surface of the mitochondrial inner membrane of Saccharomyces cerevisiae.,” *Molecular biology of the cell*, vol. 14, no. 1, pp. 324–33, Jan. 2003.

[81] N. G. Brown, M. C. Costanzo, and T. D. Fox, “Interactions among three proteins that specifically activate translation of the mitochondrial COX3 mRNA in Saccharomyces cerevisiae.,” *Molecular and cellular biology*, vol. 14, no. 2, pp. 1045–53, Feb. 1994.

[82] A. Fiori, X. Perez-Martinez, and T. D. Fox, “Overexpression of the COX2 translational activator, Pet111p, prevents translation of COX1 mRNA and cytochrome c oxidase assembly in mitochondria of Saccharomyces cerevisiae.,” *Molecular microbiology*, vol. 56, no. 6, pp. 1689–704, Jun. 2005.

[83] A. Barrientos, D. Korr, and A. Tzagoloff, “Shy1p is necessary for full expression of mitochondrial COX1 in the yeast model of Leigh’s syndrome.,” *The EMBO journal*, vol. 21, no. 1–2, pp. 43–52, Jan. 2002.

[84] X. Perez-Martinez, S. A. Broadley, and T. D. Fox, “Mss51p promotes mitochondrial Cox1p synthesis and interacts with newly synthesized Cox1p.,” *The EMBO journal*, vol. 22, no. 21, pp. 5951–61, Nov. 2003.

[85] D. Smith, J. Gray, L. Mitchell, W. E. Antholine, and J. P. Hosler, “Assembly of cytochrome-c oxidase in the absence of assembly protein Surf1p leads to loss of the active site heme.,” *The Journal of biological chemistry*, vol. 280, no. 18, pp. 17652–6, May 2005.

[86] A. Barrientos, A. Zambrano, and A. Tzagoloff, “Mss51p and Cox14p jointly regulate mitochondrial Cox1p expression in Saccharomyces cerevisiae.,” *The EMBO journal*, vol. 23, no. 17, pp. 3472–82, Sep. 2004.

[87] J. J. Mulero and T. D. Fox, “Alteration of the Saccharomyces cerevisiae COX2 mRNA 5’-untranslated leader by mitochondrial gene replacement and functional interaction with the translational activator protein PET111.,” *Molecular biology of the cell*, vol. 4, no. 12, pp. 1327–35, Dec. 1993.

[88] N. S. Green-Willms, C. A. Butler, H. M. Dunstan, and T. D. Fox, “Pet111p, an inner membrane-bound translational activator that limits expression of the Saccharomyces cerevisiae mitochondrial gene COX2.,” *The Journal of biological chemistry*, vol. 276, no. 9, pp. 6392–7, Mar. 2001.

[89] D. M. Glerum, A. Shtanko, and A. Tzagoloff, “Characterization of COX17, a yeast gene involved in copper metabolism and assembly of cytochrome oxidase.,” *The Journal of biological chemistry*, vol. 271, no. 24, pp. 14504–9, Jun. 1996.

[90] J. Beers, D. M. Glerum, and A. Tzagoloff, “Purification, characterization, and localization of yeast Cox17p, a mitochondrial copper shuttle.,” *The Journal of biological chemistry*, vol. 272, no. 52, pp. 33191–6, Dec. 1997.

[91] D. N. Heaton, G. N. George, G. Garrison, and D. R. Winge, “The mitochondrial copper metallochaperone Cox17 exists as an oligomeric, polycopper complex.,” *Biochemistry*, vol. 40, no. 3, pp. 743–51, Jan. 2001.

[92] P. A. Cobine, L. D. Ojeda, K. M. Rigby, and D. R. Winge, “Yeast contain a non-proteinaceous pool of copper in the mitochondrial matrix.,” *The Journal of biological chemistry*, vol. 279, no. 14, pp. 14447–55, Apr. 2004.

[93] M. H. Barros, A. Johnson, and A. Tzagoloff, “COX23, a homologue of COX17, is required for cytochrome oxidase assembly.,” *The Journal of biological chemistry*, vol. 279, no. 30, pp. 31943–7, Jul. 2004.

[94] M. P. Nobrega, S. C. B. Bandeira, J. Beers, and A. Tzagoloff, “Characterization of COX19, a widely distributed gene required for expression of mitochondrial cytochrome oxidase.,” *The Journal of biological chemistry*, vol. 277, no. 43, pp. 40206–11, Oct. 2002.

[95] Y.-C. Horng, P. A. Cobine, A. B. Maxfield, H. S. Carr, and D. R. Winge, “Specific copper transfer from the Cox17 metallochaperone to both Sco1 and Cox11 in the assembly of yeast cytochrome C oxidase.,” *The*

Journal of biological chemistry, vol. 279, no. 34, pp. 35334–40, Aug. 2004.

[96] M. H. Barros and A. Tzagoloff, “Regulation of the heme A biosynthetic pathway in Saccharomyces cerevisiae.,” *FEBS letters*, vol. 516, no. 1–3, pp. 119–23, Apr. 2002.

Chapter 2

ATP1 as a suppressor of the non-fermentable carbon source defects of *coa1*∆

1. Abstract

The assembly of cytochrome c oxidase (COX) in yeast mitochondria is dependent on the assembly factor Coa1. In our study, *ATP1* was identified as a suppressor of the *coa1*∆ respiration defect. Overexpression of *ATP1* improves COX activity, but did not affect bc1 complex activity or ATP synthase activity or copper levels in mitochondria of *coa1*∆ cells. *ATP1* is additive with previously discovered suppressors, *MSS51, COX10, MDJ1*. *ATP1* is additive with *MSS51 and COX10* suggests *ATP1* functions via different pathway not affecting Cox1 translation or heme *a* insertion. Interestingly, *ATP1* has a more profound effect on total oxygen consumption than COX activity alone. Using biochemical and microscopic approaches we found that *ATP1* rescues a previously unrecognized mitochondrial biogenesis defect in *coa1*∆. This defect is evident as low total mitochondrial numbers and a morphology defect with a majority of cells showing a punctate morphology. Confocal microscopy shows reduced mitochondrial volume per cell in *coa1*∆ and induction of *ATP1* expression rescued this and the wild-type tubular morphology. *ATP1* overexpression did not rescue the closely related assembly factor mutant *shy1*∆. Mitochondrial morphology and biogenesis is dependent on intact mitochondrial ultrastructure. Mutations in the MINOS complex disrupt inner membrane structure. *ATP1* and *COA1* were found to be able to rescue *aim37*∆*,* a member of the MINOS complex. While Coa1 may not be expected to influence MINOS function in cristae junction formation it help facilitate

improved loading of COX into cristae and therefore rescue the *aim37*Δ defect. We propose the rescue of respiration in *coa1*Δ by multi-copy *ATP1* is due to increased mitochondrial biogenesis perhaps due to improved inner membrane organization in *coa1*Δ or improved localization of COX to cristae.

2. Introduction

The electron transport chain in mitochondria is required for eukaryotic respiration to produce ATP. There are four electron-transporting multiprotein complexes and the ATP synthase. The electrons from reduced electron carrier (NADH and $FADH_2$) are transported by complex I-IV to molecular oxygen. As a result of this electron transportation process, water and a proton gradient were generated. The proton gradient is used by ATP synthase to produce ATP. Most mitochondrial proteins are encoded by nuclear genes including most subunits of the electron transport chain. These proteins are synthesized on cytosolic ribosomes and then transported into mitochondria by dedicated protein translocases [1] [2] [3][4]. But, there are a small number of mitochondrial proteins, eight in the yeast *Saccharomyces cerevisiae* and 13 in humans, that are encoded by mitochondrial DNA [5][6][7][8]. Except for *VAR1*, all of these mitochondrial DNA encoded proteins are subunits of the electron transport chain complexes and are inserted into the inner membrane [9][10]. Apart from complex II, which only contains nuclear DNA encoded subunits, all of the other electron transport chain complexes are formed by nuclear and

mitochondria encoded proteins.

Cytochrome c oxidase (COX) is the complex IV of the electron transport chain. The enzyme is embedded within the inner membrane (IM) with a portion of the molecule protruding into the intermembrane space (IMS) and another portion extending into the matrix compartment [11]. Eukaryotic COX is formed by 12-13 subunits. Among them, three mitochondria encoded subunit Cox1, Cox2 and Cox3 form the catalytic core of the enzyme. The other subunits integrated in the COX are encoded by the nuclear genome. They function to stabilize the enzyme by surrounding cofactor containing subunits [12]. There are three copper atoms and two heme a, which is specific to COX, in the core of the enzyme [12].

Cox1 is a mitochondrial-encoded subunit that binds heme a and the heme a3:CuB co-factors required for catalysis. Assembly of COX in *S. cerevisiae* is dependent on at least 30 different factors. The assembly process is further complicated by dual functions of some these different proteins. Translation and assembly of Cox1 is controlled by Pet 309, Mss51, Shy1, Cox14 and Coa1-4 [11] [13][14][15] (Fig.1.xxxxB). Coa1 coordinates the protein complexes involved in the transition from translation to cofactor insertion. *S. cerevisiae* lacking *COA1* are respiratory deficient. Initial genetic screens for suppressors of the respiration defect identified *MSS51*, *COA2* and *COX10* as suppressors [11]. Additionally *coa1*Δ has a mitochondrial copper defect. Culturing in high copper reverses the copper deficit and enhances respiration. Previous

investigations of *coa1*Δ were either high-copy suppressor screens or proteomics approach. We screened the *coa1*Δ in an attempt to resolve other roles for Coa1 in mitochondria.

The electron transport chain generates the proton gradient used by ATP synthase to produce ATP. The ATP synthase complex consists of F_o domain, responsible for proton translocation and F_1 domain, which catalyzes ATP synthesis [16][17][18]. Its function in producing ATP has been extensively studied, and recently the second function for morphology and organization of the inner membrane has been discovered [19][20][21][22][23]. The bulk of the mitochondria inner membrane forms cristae while the inner boundary membrane aligns the outer membrane to form the double membrane layer structure of mitochondria. There is a short tubular connection between the inner boundary and the cristae membrane called the cristae junction. The formation of the cristae tip is thought to be dependent on the positive curvature generated by ATP synthase.

The most common form of ATP synthase is monomer or homodimer [24][25][26]. In some organisms, the ATP synthase homodimers form higher oligomers [27][28]. The ATP synthase homodimers can form ribbons in the cristae membrane, which affect the physical properties of the lipid bilayer [29][30].

In *S. cerevisiae*, many proteins function in the dimerization of ATP synthase, such as Atp20, Atp21, Atp19 and Atp18. These ATP synthase

subunits associate to the F_0 portion to help form or stabilize the dimer [24][31][32][33]. Proper ultrastructure of the mitochondrial inner membrane is dependent on an antagonism between Atp20/Atp21 and Fcj1 (formation of cristae junction 1). Fcj1 was suggested to destabilize ATP synthase oligomer which would affect mitochondrial cristae [30]. Fcj1 belongs to a group of proteins that affect mitochondrial cristae. This group of proteins is called MINOS (Mitochondrial inner membrane organizing system).

3. Materials and methods

Bacterial strains

NEB 10-beta Competent *Escherichia coli* cells (High Efficiency) were used as the bacterial host for genomic library plasmid. NEB 5-alpha Competent *Escherichia coli* cells (Subcloning Efficiency) were used for general plasmid transformation.

Yeast Strains

The *S. cerevisiae* BY4743 Δ*COA1* strain was used for the construction of the genomic library and the *S. cerevisiae* BY4743 Δ*COA1* strain was also used as a recipient strain in complementation experiments. The *S. cerevisiae* DY150 Δ*COA1* strain was used as a recipient strain of the suppressors we found during the genomic library screening.

DNA manipulations

The genomic DNA was extracted manually with traditional method and can be purified by some genomic DNA clean kit. For plasmid isolation from E. coli and yeast, a Qiaprep Spin Miniprep Kit was used. For plasmid isolation from yeast, the protocol was modified: after resuspending yeast cells in 250ul kit P1 buffer, add 50-100ul of acid-washed glass beads (Sigma G-8772) and vortex for 5min. Let stand to allow the beads to settle. Transfer supernatant to a fresh 1.5 ml microcentrifuge tube. Then proceed to the 250ul kit P2 buffer step and finish the left isolation steps in the kit protocol for E. coli cells.

Genomic library preparation

The genomic library was prepared as described elsewhere [34]. The plasmid pRS413 was cut with EcoRV and treated with alkaline phosphatase (New England Biolabs). The *S. cerevisiae* BY4743 Δ*COA1 cell* genomic DNA was partially digested with EcoRV to give a maximum number of DNA fragments in the 3-10 kb size range. Then run these DNA fragments on an agarose gel, cut the DNA smear range from 3-10kb out of the gel and extract with a gel extraction kit. The genomic DNA fragments extracted and the treated pRS413 vector were ligated with T4 DNA ligase (New England Biolabs) at 14 ℃ overnight. The ligation mixture was used to transform NEB 10-beta Competent *Escherichia coli* cells (High Efficiency) with electroporation method. The transformants were selected on LB plates with ampicillin. Then the

transformants were scraped off with liquid LB medium and used to extract the genomic library plasmid with a Qiaprep Spin Miniprep Kit.

As for the number of colonies we collected, we used the genomic library construction formula:

$$\mathrm{N} = \frac{\ln(1-p)}{\ln(1-\frac{i}{g})}$$

g = genome size

i = insert size

p = probability that any point in the genome will occur at least once in the library

N = number of clones in the library

The calculation is as following:

The genome size (g) of S. cerevisiae is about 13.5Mb; Because the average gene size of S. cerevisiae is 1.5kb (most genes < 5kb; the longest < 10kb), the genomic DNA was partially digested to average size of 6kb (3kb-10kb). So the insert size (i) =6X10^3; Set the probability that any point in the genome will occur at least once in the library (P) =99%

$$\mathrm{N} = \frac{\ln(1-p)}{\ln(1-\frac{i}{g})} = \frac{\ln(1-99\%)}{\ln(1-\frac{6\times10^3}{13.5\times10^6})} = 10359$$

Genomic library Screening

After extracting the genomic library plasmid, the *S. cerevisiae* BY4743 Δ*COA1* strain was used as a recipient strain in complementation experiments with electroporation method. The transformants were first selected on synthetic complete glucose agar plates minus histidine (SCD-his). In order to have a high confident that our selection includes all genes in the genome, it's necessary to transform and collect enough transformants on the SCD-his plates according to the formula. Then, transfer the transformants from SCD-his plates to synthetic complete glycerol agar plates minus histidine (SCG-his) by replicating plates. Keep screening the extracted genomic library plasmid until find the target gene.

4. Results

ATP1 is a multi-copy suppressor of *coa1*Δ

COA1 deletion in *S. cerevisiae* results in defect on non-fermentable carbon source due to loss of COX activity [11]. A low-copy library was constructed from a *coa1*Δ strain and was screened for the ability to recue glycerol growth of *coa1*Δ. Six suppressors were isolated that rescued growth. Five contained *MSS51* while one contained a fragment that encoded *ATP1.* The suppression of glycerol growth and respiration was tested in comparison to known suppressors by growth and oxygen consumption (Fig. 2.1). The growth test suggests that *ATP1* can suppress the respiration deficiency of *coa1*Δ strain as other suppressors, such as *MSS51*, *MDJ1* and *COX10* (Fig. 2.1A). The

oxygen consumption confirmed this suppression phenotype. Moreover, *ATP1* suppression strain has higher oxygen consumption compared to *MSS51* suppression strain (Fig. 2.1B). To make sure, this suppression by *ATP1* is not due to some characteristics of the BY4743 strain, we transformed *ATP1* to an independent laboratory strain background DY150 strain and the suppression is reproducible (Data not shown).

ATP1 improved COX activity and stabilized Cox2, but didn't rescue Cu defect and *shy1*Δ deficiency

Since *ATP1* was confirmed as a suppressor of *coa1*Δ，to characterize its suppression mechanism, we first did COX activity assay and western blot to check whether *ATP1* has some direct impact on this electron transport chain complex. The COX activity assay suggests *ATP1* improved COX activity (Fig. 2.2A) and rescued the stability of Cox2 (Fig. 2.2B). We also assayed the bc1 complex (complex III) of electron transport chain. *ATP1* didn't significantly changed bc1 complex activity (Fig. 2.2C).

Yeast cells lacking *COA1* have a mitochondrial copper defect and culturing in high copper reverses the copper deficit and enhances respiration [11]. Therefore, we analyzed mitochondria metal content via inductively coupled plasma optical emission spectroscopy (ICP-OES) to check whether the copper level has been improved by *ATP1.* The result suggests *ATP1* did not change the Cu levels in the coa1Δ mitochondria (Fig. 2.2D). There is a similar complex

IV deficiency in the yeast strain *shy1*Δ including disruption of an equivalent step in COX assembly and a copper deficiency. Growth test suggests *shy1*Δ cannot be suppressed by *ATP1* (Fig. 2.3).

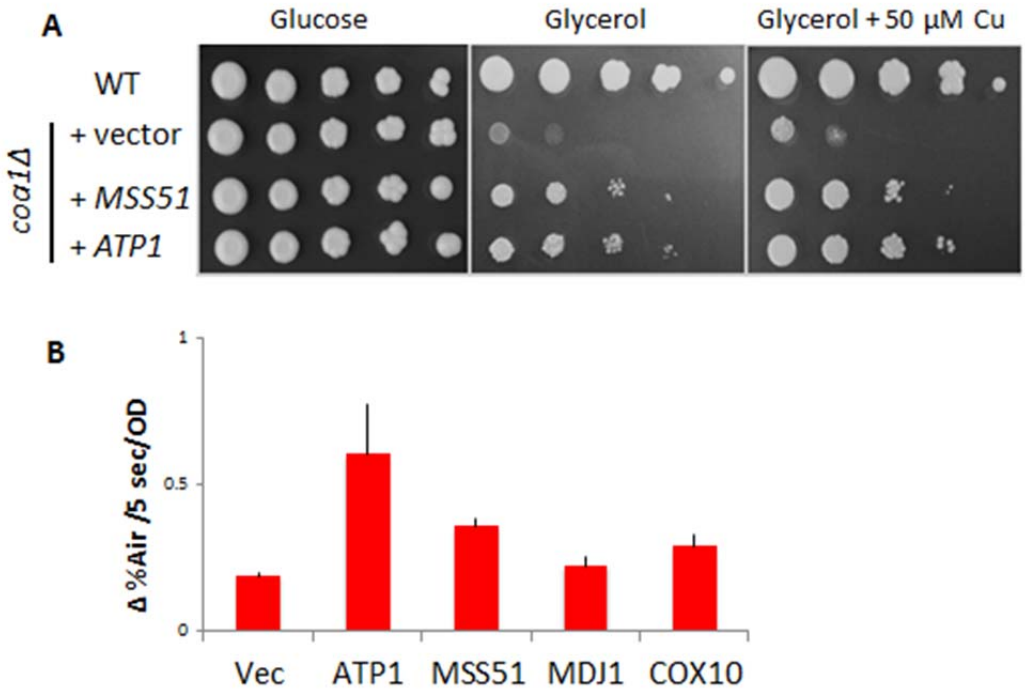

Figure 2.1: *ATP1* is a multi-copy suppressor of *coa1*Δ (A) *coa1*Δ cells transformed with suppressor MSS51 and ATP1 were grown in SC-2% glucose, serially diluted and spotted on SC-2% glucose or SC-2% glycerol with selection. The plate were incubated at 30℃for phenotypes. (B) *coa1*Δ cells with empty vector (vec) or suppressors were grown in SC-2% glucose with selection and assayed for oxygen consumption.

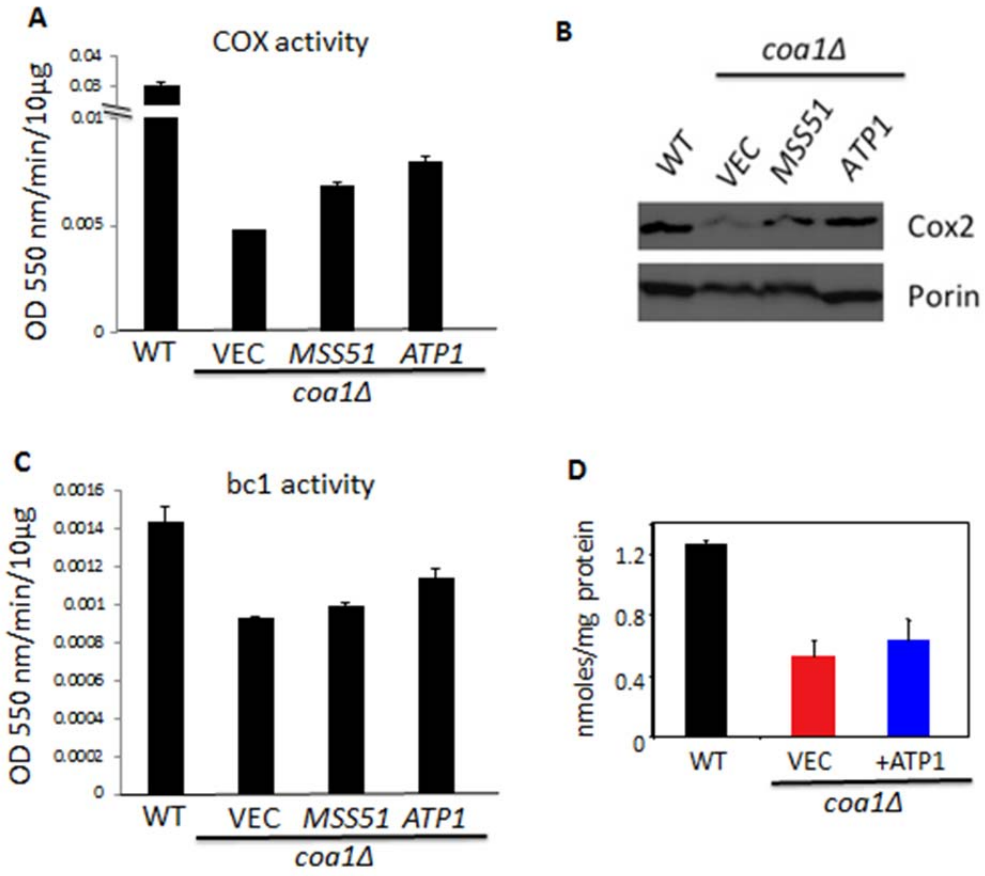

Figure 2.2: *ATP1* improved COX activity and stabilized Cox2, but didn't rescue Cu defect (A) *coa1*Δ cells with empty vector (vec) or suppressors were grown in SC-2% glucose with selection. Mitochondria were purified from these cells and assayed for COX activity. (B) Immunoblot of mitochondria from *coa1*Δ cells containing an empty vector (vec), suppressor *MSS51*, suppressor *ATP1*. (C) Mitochondria were purified from these cells and assayed for bc1 complex activity. (D) Copper levels were assessed by ICP-OES in Nycodenz-purified mitochondria of *coa1*Δ cells with empty vector (vec) or suppressor *ATP1*, and the isogenic WT BY4743.

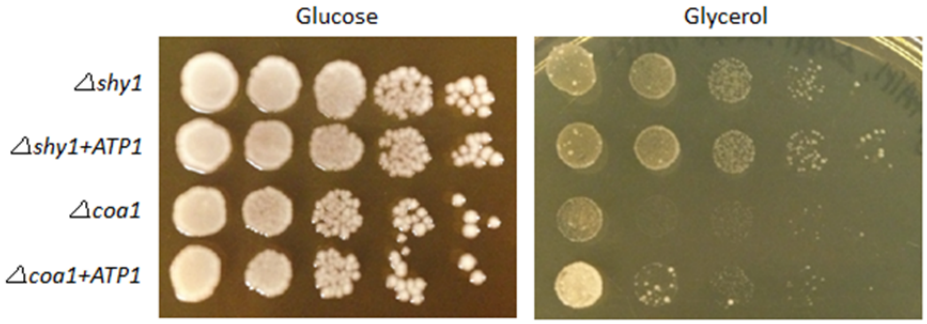

Figure 2.3: *ATP1* didn't rescue *shy1*Δ *cells* defect. *shy1*Δ expressing an empty vector and multiple copy suppressor *ATP1* were grown in SC-2% glucose, serially diluted and spotted on SC-2% glucose or SC-2% glycerol with selection. The plate were incubated at 30℃.

ATP1 changed ATP synthase activity in *coa1*∆

Since *ATP1* encodes the alpha subunit of mitochondrial ATP synthase, we assayed ATP synthase activity in *coa1*∆ plus or minus *ATP1*. *ATP1* changed ATP synthase activity in the *coa1*∆ (Fig. 2.4A). Cells lacking *COA1* do appeared to have an increase in ATP synthase activity (Fig. 2.4A). The increase may be related to mitochondrial copper deficiency as media supplementation with copper did marginally inhibit ATP synthase activity (Fig.2.4B) and copper deficiency has been reported to affect ATP synthase.

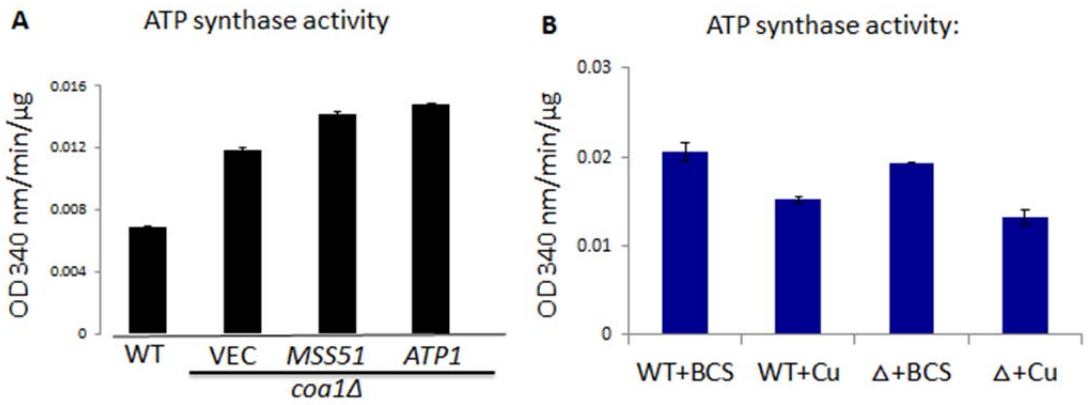

Figure 2.4: *ATP1* changed ATP synthase activity in *coa1*Δ. (A) WT cell and *coa1*Δ cells with empty vector (vec) or suppressors were grown in SC-2% glucose with selection. Mitochondria were purified from these cells and assayed for ATP synthase activity. (B) *coa1*Δ cells and isogenic WT cells were grown in SC-2% glucose plus or minus copper medium. Mitochondria were purified from these cells and assayed for ATP synthase activity.

ATP1 is additive with previously discovered suppressors

Initial genetic screens for suppressors of the *coa1*Δ respiration defect identified *MSS51*, *COA2* and *COX10* as suppressors and it was shown that *COX10* had a strong synergistic effect in combination with *MSS51* in *coa1*Δ [11]. Also the combination of *MSS51* and *COX10* enhances respiratory growth in *shy1*Δ [11]. According to this, we chose to investigate whether *ATP1* could act synergistically with the previous suppressors. We cloned these suppressors into different vectors and transformed into *coa1*Δ cells in a combination (Fig.2.5A). The results suggest that *ATP1* is additive with these previously discovered suppressors. The additive effect between *ATP1* and *MSS51* for growth is confirmed by oxygen consumption (Fig. 2.5B).

ATP1 significantly increased the mitochondrial content in *coa1*Δ

ATP synthase has been implicated in mitochondria morphology and biogenesis. The western blot analysis of mitochondrial marker porin (Por1) compared to the cytosolic marker 3-PhosphoGlycerate Kinase (Pgk1) from *coa1*Δ and WT whole cells suggested possibly reduced number of mitochondria (Fig. 2.6A). We transformed *coa1*Δ with matrix-targeted GFP which allowed for direct measurement of mitochondrial levels. The mtGFP confirmed that *coa1*Δ had reduced mitochondrial contant and *ATP1* significantly increased mitochondrial numbers based on direct measurement (Fig. 2.6B). The level of mt-GFP signal was not affected by extracellular Cu

concentrations (Fig. 2.6C). In addition, we found that *MSS51* did not increase mitochondrial numbers which suggests that *ATP1* and *MSS51* function in different ways. The mitochondrial levels in *shy1*Δ were normal and unaffected by *ATP1* expression (Fig.2.6B).

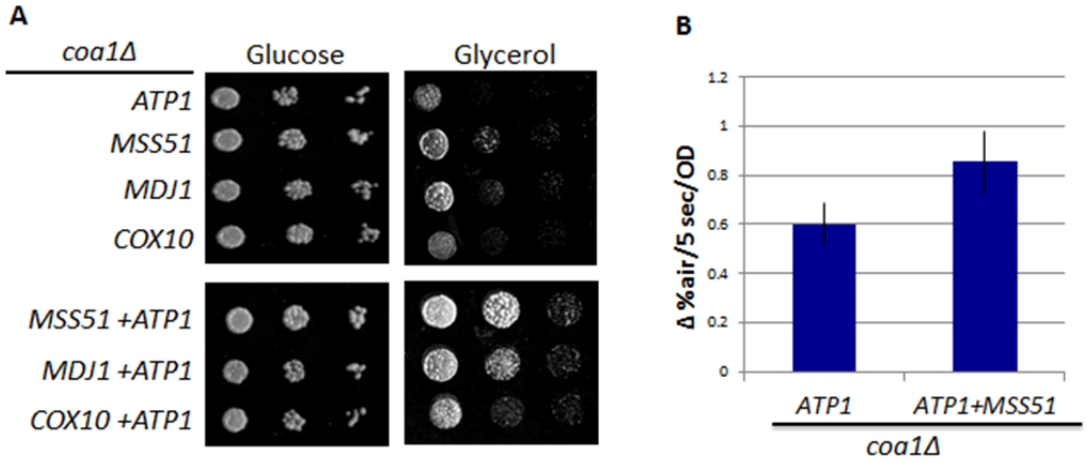

Figure 2.5: *ATP1* is additive with previous discovered suppressors (A) *coa1*Δ cells expressing single suppressors or double suppressors were grown in SC-2% glucose, serially diluted and spotted on SC-2% glucose or SC-2% glycerol with selection. The plate were incubated at 30℃for phenotypes. (B) These cells were assayed for oxygen consumption.

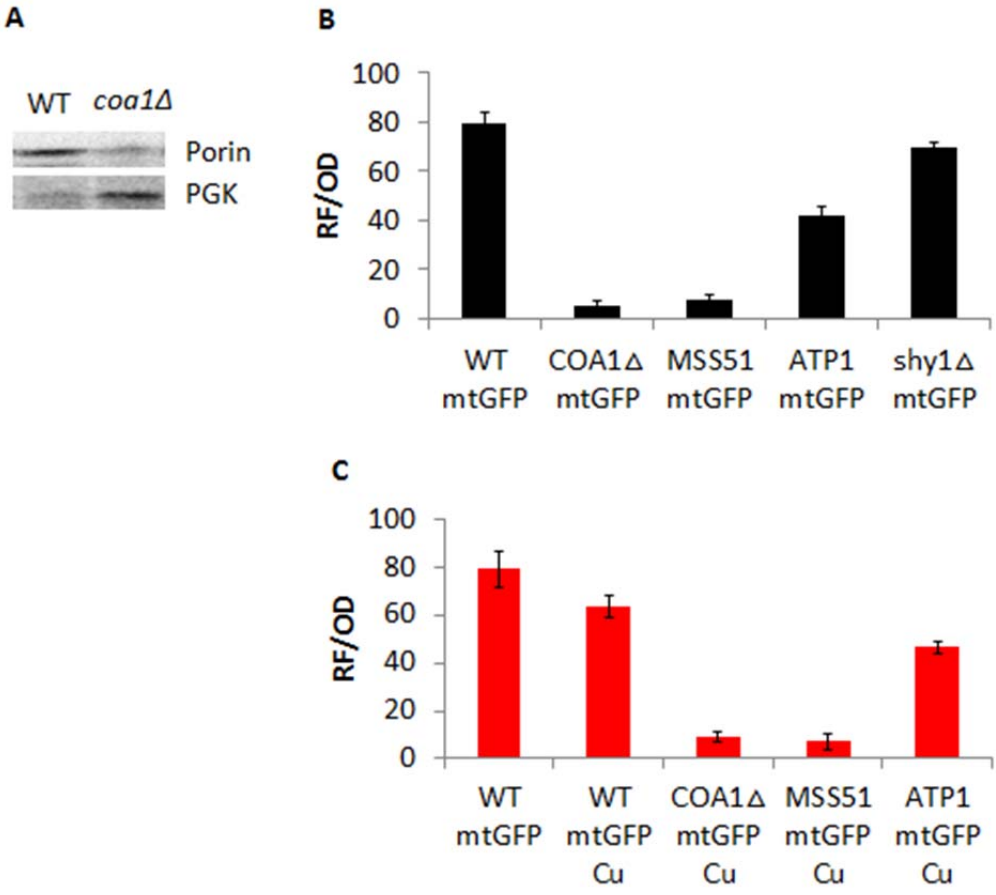

Figure 2.6: *ATP1* significantly increased the mitochondrial content in *coa1*Δ (A) Immunoblot of mitochondrial marker porin and cytosolic marker PGK1 from *coa1*Δ cells and isogenic WT cells. (B) WT cells, *coa1*Δ cells with empty vector or suppressor and *shy1*Δ cells were all transformed with matrix-targeted GFP and grown in SC-2% glucose with selection. Mitochondrial levels of these cells were assessed by measuring the green fluorescence via a fluorometer. The mitochondrial levels of these cells are also measured in the same medium with copper added.

ATP1 rescues a morphology defect in *coa1*Δ

Since *ATP1* significantly increased the mitochondrial content in *coa1*Δ, we chose to use fluorescence microscopy to visualize mitochondria in *coa1*Δ. We found that the mitochondria in *coa1*Δ were punctate and rarely if ever found as extended tubular form. *ATP1* expression induced more intense signal and the tubular morphology (Fig. 2.7). Confocal microscopy shows reduced mitochondrial volume per cell in *coa1*Δ. All these suggest that *ATP1* rescues a morphology defect in *coa1*Δ.

ATP1 and *COA1* can rescue MINOS deletion mutants

Protein-protein interaction studies had revealed possible connection between COX-Coa1-MINOS-ATP synthase [35] (Fig. 2.8B). We tested MINOS mutants for rescue by *ATP1* or *COA1*. *ATP1* and *COA1* appeared to enhance growth of *aim37*Δ at 18^{o}C on glycerol (Fig. 2.8A). We further tested the suppression of *aim37*Δ and *fcj1*Δ by *ATP1* and *COA1* on multiple carbon sources: glucose, acetate, ethanol, pyruvate, citrate, lactate at 18^{o}C and 30^{o}C. *ATP1* and *COA1* rescued growth defect of *aim37*Δ on all media. The strongest suppressions are on acetate medium and lactate glycerol with copper depleted medium (Fig. 2.9A). The oxygen consumption confirmed this suppression (Fig. 2.9B). Since the strongest suppressions are with acetate or lactate-glycerol carbon sources, we chose to test if the suppression of *aim37*Δ and *fcj1*Δ by *ATP1* and *COA1* was dependent on copper. The growth test suggests *ATP1* can significantly

rescue the growth defect of *aim37*Δ acetate with copper depletion at 18^{o}C (Fig. 2.10).

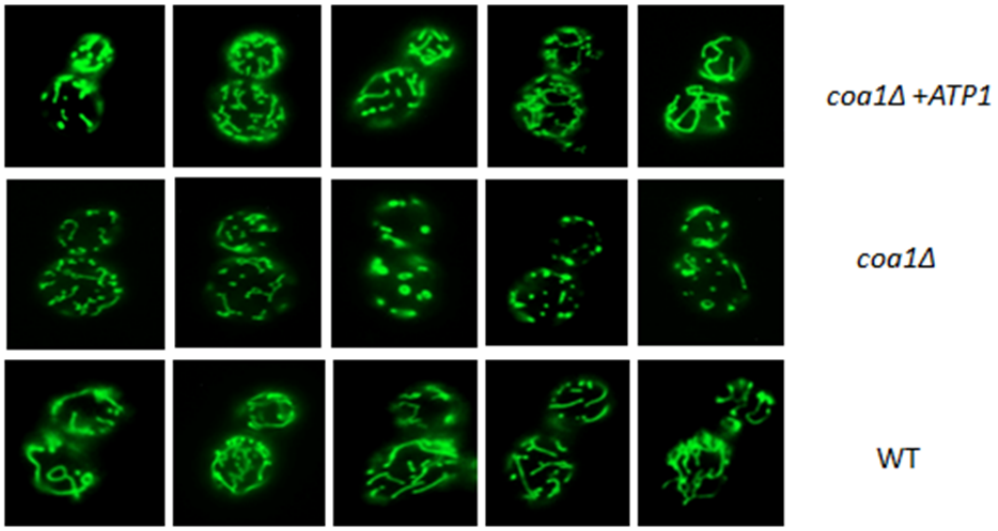

Figure 2.7: *ATP1* rescues a morphology defect in *coa1*Δ. WT cells, *coa1*Δ cells with empty vector or suppressor *ATP1* were all transformed with matrix-targeted GFP and grown in SC-2% glucose with selection. Fluorescence microscopy was used to visual mitochondria in these cells.

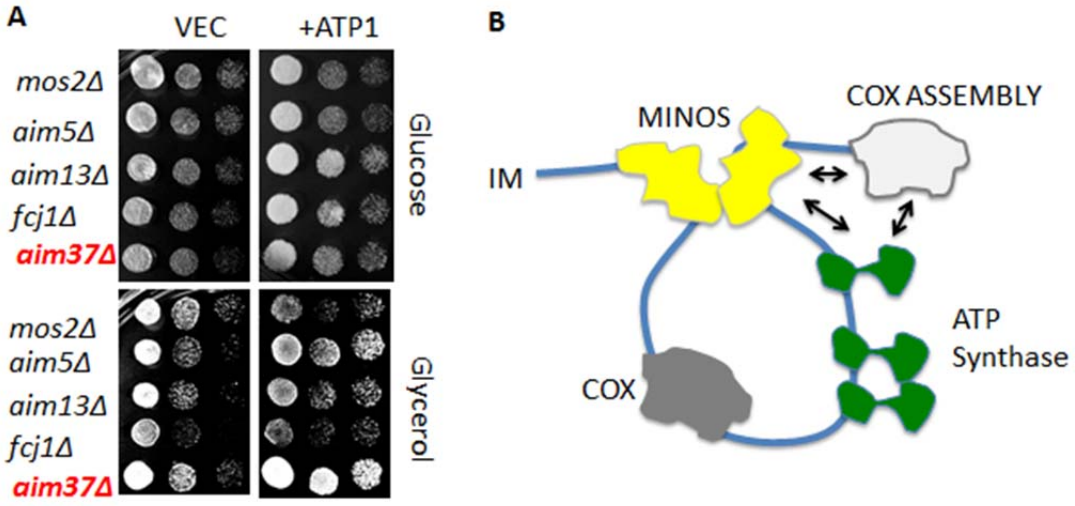

Figure 2.8: *ATP1* and *COA1* can rescue MINOS deletion mutants. (A) MINOS deletion mutants with empty vector (vec) or suppressors were grown in SC-2% glucose, serially diluted and spotted on SC-2% glucose or SC-2% glycerol with selection. The plate were incubated at 18℃for phenotypes. (B) Interaction among MINOS, ATP synthase and COX.

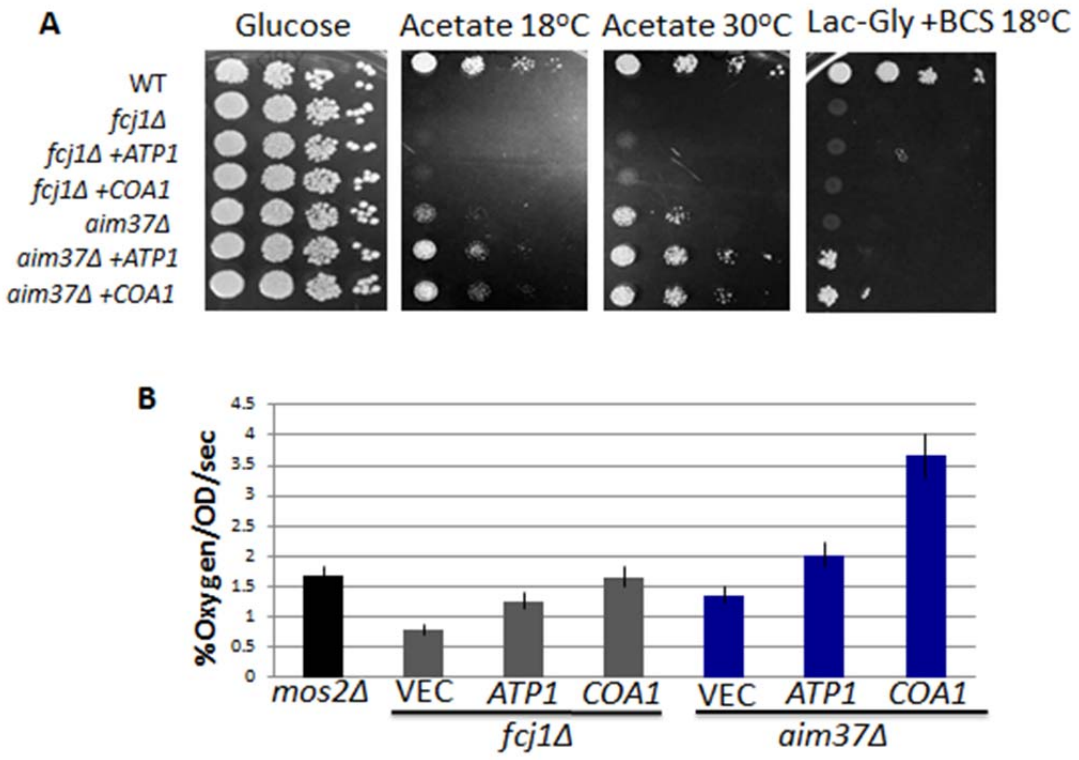

Figure 2.9: *aim37*Δ and *fcj1*Δ were screened on multiple carbon sources (A) *aim37*Δ and *fcj1*Δ with empty vector (vec) or suppressors were grown in SC-2% glucose, serially diluted and spotted on multiple carbon sources: Glucose, acetate, ethanol, pyruvate, citrate, and lactate with selection. The plate were incubated at 18℃and 30°C for phenotypes. (B) These cells were assayed for oxygen consumption.

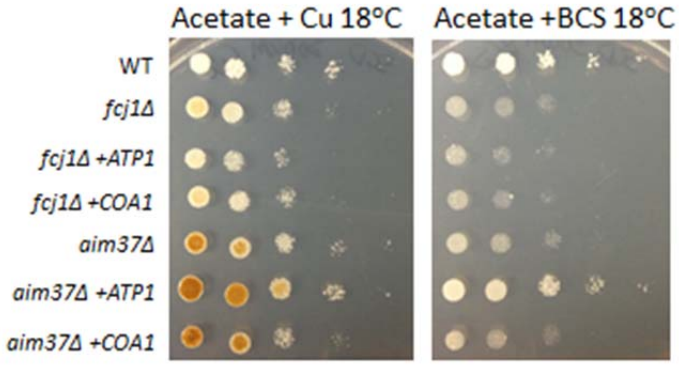

Figure 2.10: *aim37*Δ and *fcj1*Δ with empty vector (vec) or suppressors were grown in SC-2% glucose, serially diluted and spotted on acetate plus or minus copper medium. The plate were incubated at 18℃ for phenotypes.

5. Discussion

We identified *ATP1* as a suppressor of the *coa1*∆ respiration defect. Initial genetic screens for suppressors of the *coa1*∆ respiration defect identified *MSS51*, *COA2* and *COX10* as suppressors [11]. *MSS51* encodes a protein required for the translation and insertion of Cox1, while *COA2* encodes a protein that protects the initial early intermediates from degradation by Oma1, *COX10* encodes a protein that is required for modification of heme to the COX specific heme. *COX10* and *MSS51* had a strong synergistic effect in rescuing the *coa1*∆ *defect.* The combination of *MSS51* and *COX10* also enhances respiratory growth in *shy1*∆ [11]. This suggested that Coa1 had a role in the coordination of cofactor recruitment and assembly. Our result suggests *ATP1* is additive with previously discovered suppressors. The result suggests ATP1 is contributing to enhance activity via a different pathway not affecting Cox1 translation like *MSS51* or heme insertion (Fig.2.5A). There is no known assembly role for ATP synthase or the F_1 sector proteins has been described in COX assembly. While overexpression of *ATP1* appeared to improve COX activity per mitochondria it did not return the activity to WT levels. In addition *ATP1* did not significantly change bc1 complex activity or ATP synthase activity or rescue the Cu defect of *coa1*∆ cells. It should be noted that yeast requires only 30% of WT levels of COX to grow efficiently of non-fermentable carbon sources. Therefore, it is proposed that *ATP1* rescues an additional phenotype of *coa1*∆.

ATP1 did significantly change *coa1*Δ total oxygen consumption per cell. If it did not change the electron transport chain complex activity per mitochondria, we proposed that it changed at the levels of mitochondria at a whole cell level. The biochemical and cell biology approaches taken suggest that there is a previously unrecognized mitochondrial biogenesis defect in this *coa1*Δ background. This defect included a low total mitochondrial number and an apparent punctate morphology defect. Both phenotypes could be rescued by *ATP1*. The defect in morphology is most likely closely related to the biogenesis defect with failure to mix contents of mitochondria leading to decrease in membrane potential and prevent biogenesis. However, membrane potential was unchanged in the WT, coa1Δ or suppressed versions of coa1Δ, therefore we decide to investigate more direct role in morphology.

To confirm that the phenotype was not a function of lack of COX we tested the closely related mutant *shy1*Δ. Consistent with a prediction that Coa1 may have a more direct role in morphology, shy1 had no defect in mitochondrial numbers assessed by mt-GFP and *ATP1* cannot rescue a *shy1*Δ growth on non-fermentable carbon sources (Fig.2.3). Deletion of *SHY1* result copper deficit but does not share the same biogenesis defect highlighting the unique role of Coa1 and also decreasing the probability that copper deficit was involved in this phenotype.

The morphology of the mitochondria, the formation of tubular structure is dependent on the mitochondrial cristae junction. The cristae junctions are

formed through the activity of the MINOS complex [30][36][35][37]. This complex contains numerous proteins including Fcj1. A proteomic study suggested ATP synthase may interact with MINOS complex in the formation of cristae junction. The mitochondrial inner membrane organization complex (MINOS) is required for in cristae junction formation in yeast and one study annotated connection between COX assembly proteins, ATP synthase and (MINOS) [36], we pursued this as a possible basis for the mitochondrial biogenesis defect. We show genetic rescue of MINOS defects in *AIM37* a MINOS complex member with *ATP1* and *COA1.* Previous protein-protein interaction study suggests Atp1 is the only ATP synthase subunit that was immunoprecipitated along with Aim37 [35]. While Coa1 may not be expected to influence MINOS function in cristae junction formation it may help facilitate improved loading of fully assembled COX into cristae. Proteolysis checkpoints in COX assembly occur in the boundary membrane of mitochondria therefore Coa1 may be functioning to prevent the partially assembled COX from entering cristae. *COA2* another suppressor of *coa1*∆ is also involved in regulating the proteolysis of transient complexes of Cox1 during assembly. Failure to insertion Cox into the cristae or failure to form cristae should result in similar phenotypes, suboptimal growth on non-fermentable carbon sources. Therefore Coa1-Atp1 connection may be via facilitated insertion of assembled COX in cristae.

In conclusion, a new phenotype of cells lacking *COA1* was discovered, a

mitochondrial morphology/biogenesis defect and we propose that the rescue of respiration in *coa1*Δ by multi-copy *ATP1* is due to correction of this defect perhaps due to improved inner membrane organization or improved localization of COX to cristae.

6. Reference

[1] R. E. Jensen and C. D. Dunn, “Protein import into and across the mitochondrial inner membrane: role of the TIM23 and TIM22 translocons.,” *Biochim. Biophys. Acta*, vol. 1592, no. 1, pp. 25–34, Sep. 2002.

[2] C. M. Koehler, “New developments in mitochondrial assembly.,” *Annu. Rev. Cell Dev. Biol.*, vol. 20, pp. 309–35, Jan. 2004.

[3] P. Rehling, K. Brandner, and N. Pfanner, “Mitochondrial import and the twin-pore translocase.,” *Nat. Rev. Mol. Cell Biol.*, vol. 5, no. 7, pp. 519–30, Jul. 2004.

[4] W. Neupert and J. M. Herrmann, “Translocation of proteins into mitochondria.,” *Annu. Rev. Biochem.*, vol. 76, pp. 723–49, Jan. 2007.

[5] A. Tzagoloff and A. M. Myers, “Genetics of mitochondrial biogenesis.,” *Annu. Rev. Biochem.*, vol. 55, pp. 249–85, Jan. 1986.

[6] L. A. Grivell, M. Artal-Sanz, G. Hakkaart, L. De Jong, L. G. Nijtmans, K. Van Oosterum, M. Siep, and H. Van Der Spek, “Mitochondrial assembly in yeast.,” *FEBS Lett.*, vol. 452, pp. 57–60, 1999.

[7] S. DiMauro and E. A. Schon, “Mitochondrial respiratory-chain diseases.,” *N. Engl. J. Med.*, vol. 348, no. 26, pp. 2656–68, Jun. 2003.

[8] F. Fontanesi, I. C. Soto, D. Horn, and A. Barrientos, “Assembly of mitochondrial cytochrome c-oxidase, a complicated and highly regulated cellular process.,” *Am. J. Physiol. Cell Physiol.*, vol. 291, no. 6, pp. C1129–47, Dec. 2006.

[9] R. Stuart, “Insertion of proteins into the inner membrane of mitochondria: the role of the Oxa1 complex.,” *Biochim. Biophys. Acta*, vol. 1592, no. 1, pp. 79–87, Sep. 2002.

[10] J. M. Herrmann and S. Funes, “Biogenesis of cytochrome oxidase-sophisticated assembly lines in the mitochondrial inner membrane.,” *Gene*, vol. 354, pp. 43–52, Jul. 2005.

[11] F. Pierrel, M. L. Bestwick, P. A. Cobine, O. Khalimonchuk, J. A. Cricco, and D. R. Winge, “Coa1 links the Mss51 post-translational function to Cox1 cofactor insertion in cytochrome c oxidase assembly.,” *EMBO J.*, vol. 26, no. 20, pp. 4335–46, Oct. 2007.

[12] T. Tsukihara, H. Aoyama, E. Yamashita, T. Tomizaki, H. Yamaguchi, K. Shinzawa-Itoh, R. Nakashima, R. Yaono, and S. Yoshikawa, “Structures of metal sites of oxidized bovine heart cytochrome c oxidase at 2.8 A.,” *Science*, vol. 269, no. 5227, pp. 1069–74, Aug. 1995.

[13] D. U. Mick, K. Wagner, M. van der Laan, A. E. Frazier, I. Perschil, M. Pawlas, H. E. Meyer, B. Warscheid, and P. Rehling, “Shy1 couples Cox1 translational regulation to cytochrome c oxidase assembly.,” *EMBO J.*, vol. 26, no. 20, pp. 4347–58, Oct. 2007.

[14] D. U. Mick, M. Vukotic, H. Piechura, H. E. Meyer, B. Warscheid, M. Deckers, and P. Rehling, “Coa3 and Cox14 are essential for negative feedback regulation of COX1 translation in mitochondria.,” *J. Cell Biol.*, vol. 191, no. 1, pp. 141–54, Oct. 2010.

[15] M. Bestwick, O. Khalimonchuk, F. Pierrel, and D. R. Winge, “The role of Coa2 in hemylation of yeast Cox1 revealed by its genetic interaction with Cox10.,” *Mol. Cell. Biol.*, vol. 30, no. 1, pp. 172–85, Jan. 2010.

[16] P. D. Boyer, “The ATP synthase--a splendid molecular machine.,” *Annu. Rev. Biochem.*, vol. 66, pp. 717–49, Jan. 1997.

[17] R. H. Fillingame, “PROTEIN STRUCTURE: Molecular Rotary Motors,” *Science (80-.).*, vol. 286, no. 5445, pp. 1687–1688, Nov. 1999.

[18] J. Velours and G. Arselin, “The Saccharomyces cerevisiae ATP Synthase,” *J. Bioenerg. Biomembr.*, vol. 32, no. 4, pp. 383–390, Sep. 2000.

[19] M.-F. Giraud, P. Paumard, V. Soubannier, J. Vaillier, G. Arselin, B. Salin, J. Schaeffer, D. Brèthes, J.-P. di Rago, and J. Velours, “Is there a relationship between the supramolecular organization of the

mitochondrial ATP synthase and the formation of cristae?," *Biochim. Biophys. Acta*, vol. 1555, no. 1–3, pp. 174–80, Sep. 2002.

[20] P. Paumard, J. Vaillier, B. Coulary, J. Schaeffer, V. Soubannier, D. M. Mueller, D. Brèthes, J.-P. di Rago, and J. Velours, "The ATP synthase is involved in generating mitochondrial cristae morphology.," *EMBO J.*, vol. 21, no. 3, pp. 221–30, Feb. 2002.

[21] P. D. Gavin, M. Prescott, S. E. Luff, and R. J. Devenish, "Cross-linking ATP synthase complexes in vivo eliminates mitochondrial cristae.," *J. Cell Sci.*, vol. 117, no. Pt 11, pp. 2333–43, May 2004.

[22] D. Thomas, P. Bron, T. Weimann, A. Dautant, M.-F. Giraud, P. Paumard, B. Salin, A. Cavalier, J. Velours, and D. Brèthes, "Supramolecular organization of the yeast F1Fo-ATP synthase.," *Biol. Cell*, vol. 100, no. 10, pp. 591–601, Oct. 2008.

[23] J. Velours, A. Dautant, B. Salin, I. Sagot, and D. Brèthes, "Mitochondrial F1F0-ATP synthase and organellar internal architecture.," *Int. J. Biochem. Cell Biol.*, vol. 41, no. 10, pp. 1783–9, Oct. 2009.

[24] I. Arnold, K. Pfeiffer, W. Neupert, R. A. Stuart, and H. Schägger, "Yeast mitochondrial F1F0-ATP synthase exists as a dimer: identification of three dimer-specific subunits.," *EMBO J.*, vol. 17, no. 24, pp. 7170–8, Dec. 1998.

[25] L. G. J. Nijtmans, J.-W. Taanman, A. O. Muijsers, D. Speijer, and C. Van den Bogert, "Assembly of cytochrome-c oxidase in cultured human cells," *Eur. J. Biochem.*, vol. 254, no. 2, pp. 389–394, Jun. 1998.

[26] I. Wittig, J. Velours, R. Stuart, and H. Schägger, "Characterization of domain interfaces in monomeric and dimeric ATP synthase.," *Mol. Cell. Proteomics*, vol. 7, no. 5, pp. 995–1004, May 2008.

[27] H. Eubel, L. Jänsch, and H.-P. Braun, "New insights into the respiratory chain of plant mitochondria. Supercomplexes and a unique composition of complex II.," *Plant Physiol.*, vol. 133, no. 1, pp. 274–86, Sep. 2003.

[28] D. De los Rios Castillo, M. Zarco-Zavala, S. Olvera-Sanchez, J. P. Pardo, O. Juarez, F. Martinez, G. Mendoza-Hernandez, J. J. García-Trejo, and O. Flores-Herrera, "Atypical cristae morphology of human syncytiotrophoblast mitochondria: role for complex V.," *J. Biol. Chem.*, vol. 286, no. 27, pp. 23911–9, Jul. 2011.

[29] M. Strauss, G. Hofhaus, R. R. Schröder, and W. Kühlbrandt, “Dimer ribbons of ATP synthase shape the inner mitochondrial membrane.,” *EMBO J.*, vol. 27, no. 7, pp. 1154–60, Apr. 2008.

[30] R. Rabl, V. Soubannier, R. Scholz, F. Vogel, N. Mendl, A. Vasiljev-Neumeyer, C. Körner, R. Jagasia, T. Keil, W. Baumeister, M. Cyrklaff, W. Neupert, and A. S. Reichert, “Formation of cristae and crista junctions in mitochondria depends on antagonism between Fcj1 and Su e/g.,” *J. Cell Biol.*, vol. 185, no. 6, pp. 1047–63, Jun. 2009.

[31] P. Paumard, G. Arselin, J. Vaillier, S. Chaignepain, K. Bathany, J. M. Schmitter, D. Brèthes, and J. Velours, “Two ATP Synthases Can Be Linked through Subunits i in the Inner Mitochondrial Membrane of Saccharomyces cerevisiae †,” *Biochemistry*, vol. 41, no. 33, pp. 10390–10396, Aug. 2002.

[32] V. Soubannier, J. Vaillier, P. Paumard, B. Coulary, J. Schaeffer, and J. Velours, “In the absence of the first membrane-spanning segment of subunit 4(b), the yeast ATP synthase is functional but does not dimerize or oligomerize.,” *J. Biol. Chem.*, vol. 277, no. 12, pp. 10739–45, Mar. 2002.

[33] K. Wagner, I. Perschil, C. D. Fichter, and M. van der Laan, “Stepwise assembly of dimeric F(1)F(o)-ATP synthase in mitochondria involves the small F(o)-subunits k and i.,” *Mol. Biol. Cell*, vol. 21, no. 9, pp. 1494–504, May 2010.

[34] F. Rodrigues, A. M. Zeeman, C. Alves, M. J. Sousa, H. Y. Steensma, M. Côrte-Real, and C. Leão, “Construction of a genomic library of the food spoilage yeast Zygosaccharomyces bailii and isolation of the beta-isopropylmalate dehydrogenase gene (ZbLEU2).,” *FEMS Yeast Res.*, vol. 1, no. 1, pp. 67–71, Apr. 2001.

[35] S. Hoppins, S. R. Collins, A. Cassidy-Stone, E. Hummel, R. M. Devay, L. L. Lackner, B. Westermann, M. Schuldiner, J. S. Weissman, and J. Nunnari, “A mitochondrial-focused genetic interaction map reveals a scaffold-like complex required for inner membrane organization in mitochondria.,” *J. Cell Biol.*, vol. 195, no. 2, pp. 323–40, Oct. 2011.

[36] K. von der Malsburg, J. M. Müller, M. Bohnert, S. Oeljeklaus, P. Kwiatkowska, T. Becker, A. Loniewska-Lwowska, S. Wiese, S. Rao, D. Milenkovic, D. P. Hutu, R. M. Zerbes, A. Schulze-Specking, H. E. Meyer, J.-C. Martinou, S. Rospert, P. Rehling, C. Meisinger, M. Veenhuis, B. Warscheid, I. J. van der Klei, N. Pfanner, A. Chacinska, and M. van der Laan, “Dual Role of Mitofilin in Mitochondrial Membrane

Organization and Protein Biogenesis," *Dev. Cell*, vol. 21, no. 4, pp. 694–707, 2011.

[37] M. Harner, C. Körner, D. Walther, D. Mokranjac, J. Kaesmacher, U. Welsch, J. Griffith, M. Mann, F. Reggiori, and W. Neupert, "The mitochondrial contact site complex, a determinant of mitochondrial architecture.," *EMBO J.*, vol. 30, no. 21, pp. 4356–70, Nov. 2011.

Chapter 3

High-Throughout Discovery of the genetic causes of a suppression phenotype in *coa1Δ* background

1. Abstract:

Coa1 is an assembly factor for cytochrome c oxidase. We undertook an approach to isolate evolved homozygous diploid strains capable of growth on non-fermentable carbon source in the absence of *COA1*. To identify the mutations, we used the next generation sequencing. Four haploid strains (A1, A2, A3, and A4) with 2:2 segregation of non-fermentable growth were isolated from a suppressor strain (S1), sequenced separately and compared to a reference sequence. An optimized sequencing library preparation procedure was described, resulting in 4.1G data for the four strains. The sequencing data quality is very good, with 92% data with a Quality Score above 30 and the cluster passing filter (CPF) was 89.8%. The whole genome was covered very well with 99.9% covered and with an average coverage 68. The mean read length is longer than 240bp. We identified SNPs that are only present in A2 and A4, SNPs that only in A1 and A3, and all the SNPs that present in the BY4743 background. We observed a 2:2 segregation of a SNP (G→C) at 664 nucleotide position of MKK1 in A2 and A4 sequence consistent with the known sequences. In A1 and A3 sequence, we found there is a SNP in YGL260W gene, which is not present in A2 and A4. The sequencing data also confirmed a known strain-specific gene deletion and discovered a 144bp deletion mutation in *ATP2* in A1 and A3 sequence. The growth test suggests *coa1*Δ or *atp2*Δ have synthetic effect. Overexpressing YGL260W from A2 in A1 did not

improve the growth of A1 on glucose and glycerol medium. Overexpressing *ATP2* gene from A2 into A1 or A3, the growth defect on glycerol was suppressed. This means the suppression mutation in S1 separated into all the four haploid strain (A1, A2, A3 and A4). An novel mitochondrial SNP was found in *COX1*. In order to verify whether this *COX1* SNP is the mutation that suppresses the glycerol growth defect, the mitochondrial genome of the haploid strain A2, A4 and *coa1*∆ were removed to produce A2 ρ cell, A4 ρ cell and *coa1*∆ ρ cell. These cells need to be further mated with each other and growth on non-fermentable medium tested. As for the A2 and A4 haploid strain, although they are able to grow on glycerol medium, however, they grow much weaker than S1. We recapitulated the S1 growth phenotype by crossing A2 ρ cell with A1 cell. The newly generated diploid cell “A2 ρ + A1” grows as well as S1 strain on glycerol medium. Overexpressing of *ATP2* in S1 decreased the oxygen consumption of the S1 cell. Based on the superior growth of S1 compared to A2 or A4, suggesting that the heterozygous *ATP2* allele improves growth by increasing the apparent copy number of *ATP1*. We hypothesize that glycerol growth is dependent on the unique *COX1* allele.

2. Introduction

In the past, whole genome sequencing was time-consuming and expensive, and therefore its application in biological research has been limited to obtaining the reference sequence information of model organisms or humans. Development of low-cost, efficient high-throughput sequencing ("next generation" sequencing) technology, has solved some of these problems. The ability to generate the sequence of the whole genome of an organism without any reference information, or resequence a specific strain of a model organism is now feasible. There are many popular cost-effective and high through data next generation sequencing platforms, such as 454 and Illumina that make it possible to sequence a mutant with a specific phenotype.

For Illumina platform, the Nextera DNA Preparation Kit uses an engineered transposome to simultaneously fragment and tag input DNA, adding unique adapter sequences in the process. A limited-cycle PCR reaction uses these adapter sequences to amplify the insert DNA. The PCR reaction also adds index sequences on both ends of the DNA, thus enabling dual-indexed sequencing of pooled libraries on any Illumina Sequencing System. After the sample preparation, large number of DNA fragments are immobilized on a solid surface and read with fluorescent, labeled nucleotides. A wide variety of libraries can be sequenced, with average fragment sizes as small as 250 bp to as large as 1000-1500 bp. An ideal data amount of 7-8 Giga bases of sequence data can be obtained at a cost of less than $1000.

The high efficiency of next-generation sequencing platforms makes it a powerful tool for personal laboratory. In the past, it was commonly used for human genomes and other large genomes, but now it has become more and more prevalent with small genomes. One problem with small genome sequencing is that for most species, there is no reference genome. In this case, it is necessary to sequence the whole genome de novo with no reference genome. The assembly quality of genome sequences from de novo sequencing depends on the contig quality, or continuous sequences generated by aligning overlapping sequencing reads. The number of gaps in the assembled genome sequence depends on the size and continuity of the contigs. Short read lengths can lead to a lot of gaps, mismatches and poor quality data. This would be more serious in regions that have lots of repetitive sequences. Now some next-generation sequencing platforms, like Illumina MiSeq, provide paired-end sequencing. With both ends of a DNA fragment are sequenced, paired-end reads improve the alignment, especially for regions with repetitive sequences, thereby producing longer contigs. All of these improvements can help reduce gap numbers in the consensus sequence and produce a more complete coverage of the whole genome.

Sometimes even the model organism used in the research project has several strains with different strain-specific phenotypes, but detailed information about the genetic difference between these strains is unknown. Next-generation sequencing can help to identify the differences that can be

helpful with experimental design and analysis. Another advantage of getting the whole genome sequence information of a specific strain is that it can be an alternative way to discover a suppressor mutation.

But the interpretation of the sequencing data set is still difficult, because each mutant strain may contain 50-100 random mutations. Many of these mutations are background, unrelated genes, and usually needed extensive functional experiments to determine which one cause the phenotype. Therefore, the fewer the mutations, the more likely it is to identify the mutation that causes the phenotype. In this case, it's better to get the strain evolved mutant, rather than with some artificial mutagenesis. The mutant may have only 10-20 mutations per bacterial genome [1][2][3][4][5][6]. In some case, there are only as few as 3 mutations [7][8], or more than 40 [9].

The main problem of analyzing high-throughput sequencing data is how to identify the mutations that are responsible for the interested phenotype or how to filter out background mutations. Besides using strain evolved mutant, it's helpful to obtain multiple independent mutant strains from the phenotype screen, the statistics of independent selection events will quickly help distinguish the true target genes [10]. As more mutant strains are sequenced, true target genes are guaranteed by the Law of Large Numbers to rise above the background noise [10]. As for the cost of sequencing so many mutant strains, because it only want to identify the mutation that cause the interested phenotype, rather than getting the whole genome consensus sequence for

each individual strain, all the mutant strains are pooled together to be sequenced.

The assembly of cytochrome c oxidase (COX) in yeast mitochondria is complicated by interaction of numerous factors. It is known that COX assembly is dependent on the assembly factor Coa1. While multi-copy suppressors of this defect have been isolated the complete function of Coa1 is still unresolved. We undertook an approach to isolate spontaneous suppressor mutants in an evolved homozygous diploid background to perhaps uncover new components of the pathway using next generation sequencing technology. Based on all these results presented here, we designed a strategy to further identify the mutation that suppresses the *coa1⊿* defect and discussed the possible reasons for failing to discover the expected mutation by this next generation sequencing technology. The next generation sequencing experiment we executed also provides the whole genome sequence of *S. cerevisiae* BY4743 strain (combination of BY4741 and BY4742).

3. Materials and methods

Bacterial strains

NEB 10-beta Competent *Escherichia coli* cells (High Efficiency) were used as the bacterial host for genomic library plasmid. NEB 5-alpha Competent *Escherichia coli* cells (Subcloning Efficiency) were used for general plasmid transformation.

Yeast Strains and spores

The WT strain is in *S. cerevisiae* BY4743 background. The BY4743 strain comes from hybridization of BY4741 and BY4742. The *coa1⊿* strain was in the *S. cerevisiae* BY4743 background, created by disruption using KanMX. The spontaneous mutant strains S1, S2, S3 were selected by pouring *coa1⊿* cells on YPLG plates. The four spores A1, A2, A3, and A4 were dissected from S1 strain.

Prepare genomic DNA

The genomic DNA was extracted from A1, A2, A3, and A4 haploid yeast cells manually with traditional method and purified by some genomic DNA clean kit. Then the genomic DNA was serial diluted and measured the concentration by Qubit dsDNA HS Assay Kits (For use with the Qubit 2.0 Fluorometer) or KAPA Library Quantification Kits. The DNA quality was

detected by Nanodrop. If the ratio of absorbance at 260 nm and 280 nm is around 1.8, it is generally accepted as “pure” for DNA. Expected 260/230 values are commonly in the range of 2.0-2.2. The genomic DNA was also run on the agarose to check the intactness.

Nextera DNA Sample Preparation for Illumina MiSeq platform

Instead using the Illumina “Nextera DNA sample preparation guide”, we used a much simpler protocol as following:

Using:

Nextera DNA Sample Prep Kit

Nextera Index Kit

Qubit dsDNA HS Assay Kit (For use with the Qubit 2.0 Fluorometer) or KAPA Library Quantification Kit

Zymo DNA Clean and Concentrator-5

Agilent HS DNA kit (For use with Agilent Technologies 2100 bioanalyzer)

E.Z.N.A. NGS Clean-IT Kit (or use E.Z.N.A. Size Select-IT Kit)

Tagmentation of genomic DNA:

1) Thaw on ice Tagment DNA Buffer (TD) and Tagment DNA enzyme (TDE1). After thawing, ensure all reagents are adequately mixed by inverting the tubes 3-5 times, followed by a brief spin in a microcentrifuge.

Ensure the reaction is assembled in the order described for optimal kit performance.

2) Label tubes and add 20µl of genomic DNA at 2.5ng/µl (50ng total) to each tube.

To obtain a proper fragmented DNA library is very important for sequencing quality. It is recommended to use genomic DNA clean kit to purify the starting DNA first, and measure the DNA concentration using a fluorometric based method specific for double strand DNA such as the Qubit ds DNA HS Assay system or the KAPA Library Quantification system. (See specific protocol). Nanodrop should be avoided.

3) Add 25µl of TD Buffer.

4) Add 5µl of TDE1. Gently pipette up and down 10 times to mix.

5) Centrifuge at 280g at 20°C for 1min.

6) Run on PCR machine (Ensure that lid is heating during incubation) with the following program:

55°C for 5 minutes

Hold at 4°C

Clean up of tagmented DNA:

1) Thaw the Resupension Buffer (RSB) at room temperature.

2) Use Zymo DNA Clean & Concentrator-5 Kit to clean the tagmented DNA (See specific kit protocol).

3) Finally, use 25µl of RSB to elute the tagmented DNA sample.

Optional but recommended: check the products of tagmentation reaction by loading 1µl of undiluted Zymo eluate on a HS Bioanalyzer chip. This should produce a broad distribution of DNA fragments. (see Agilent HS DNA protocol). During this control keep samples on ice, do not freeze them.

PCR set up:

1) If less than of a full set of libraries is pooled for sequencing, ensure that correct index 1 (i7) and index 2 (i5) primers have been selected. See the Dual Indexing and Low Plexity Pooling Guidelines section at the end of the Nextera DNA Sample Preparation Guide.
2) Thaw at room temperature the PCR Master Mix (NPM), the PCR Primer Cocktail (PPC) and index primers.

After thawing, ensure all reagents are adequately mixed by inverting the tubes 3-5 times, followed by a brief spin in a microcentrifuge.

3) On PCR tubes, add 5 µl of index 1 primers (orange caps) and 5 µl of index 2 primers (white caps) on corresponding tubes.

To avoid index cross-contamination, discard orange and white original caps and apply new caps (same colors) provided in the kit.

4) Add 15 µl of NPM to each tube containing primers.
5) Add 5 µl of PPC to each tube containing NPM and primers.
6) Transfer 20 µl of purified tagmented DNA and gently pipette up and down

3-5 times. Close tubes.

7) Centrifuge at 280g at 20°C for 1min.

8) Run on thermocycler (Ensure that lid is heating during incubation) with the following program:

72°C for 3 min

95°C for 30 sec

5 cycles of:

98°C for 10 sec

63°C for 30 sec

72°C for 3 min

Hold at 10°C

If not plan to immediately proceed to PCR clean-up following the completion of PCR, tubes can remain on the thermal cycler overnight, or store it at 2° to 8°C up to 2 days.

PCR clean up:

1) Use E.Z.N.A. NGS Clean-IT Kit (or use E.Z.N.A. Size Select-IT Kit) to clean the PCR product (see specific protocol).

2) Finally, use 32.5 µl of RSB to elute the PCR product.

Now the sample can be kept at -20°C.

Validate library:

In order to get good quality and maximum amount of sequencing data from the MiSeq run, it's quite important to load appropriate amount of DNA libraries on the reagent cartridge of the MiSeq platform. It means there should be enough DNA library fragments being immobilized to the flow cell surface to produce enough clusters for sequencing, and at the same time, without saturating the flow cell leading to bad quality of sequencing data. The amount of DNA libraries loaded depends on the library concentration and the size distribution of the library DNA fragments.

Use Qubit dsDNA HS Assay Kit or KAPA Library Quantification Kit to quantify libraries and use Agilent Technologies 2100 bioanalyzer with HS DNA chip to check the size distribution of libraries fragments. When a HS DNA chip is not available, get the rough size distribution of library DNA fragments with a low sensitive DNA chip is still helpful for deciding how much DNA library should be loaded on the cartridge.

See the Validate Library Guidelines of the Nextera DNA Sample Preparation Guide. For illumina platform, a wide variety of libraries can be sequenced, with average fragment sizes as small as 250 bp to as large as 1000-1500 bp. For the fragments large than 1500 bp, they have difficulty to form cluster after binding on the flow cell, therefore if the libraries average size distribution got from the bioanalyzer is greater than 1000 bp, it is necessary to adjust the DNA concentration conversion formula and library DNA amount

loaded, according to the quality control table in Nextera DNA Sample Preparation Guide.

Pool and denature libraries for MiSeq run

Based on the validation results of the libraries, pool and denature the DNA libraries according to illumina protocol “Preparing DNA Libraries for Sequencing on the MiSeq”. The most important thing that should be careful with is the NaOH used for denaturing the libraries. Always prepare freshly diluted NaOH and use accurate amount. It is important that the concentration of NaOH is equal to 0.2 N in the denaturation solution and not more than 0.001 (1 mM) in the final solution after diluting with HT1. If it’s less than the designated concentration, it would be hard for double strand DNA to be denatured to single strand and further bind to the flow cell surface. On the other hand, if it’s higher than the designated concentration, it will finally prevent the formation of the cluster on the flow cell. Both conditions will affect the cluster formation and decrease the sequencing data amount finally got.

4. Results and Discussion

Spontaneous mutants of *coa1Δ* were isolated

Three spontaneous mutants of *coa1Δ* were isolated on glycerol plate and named S1, S2 and S3. The growth test suggests the respiration deficiency of *coa1Δ* has been suppressed in these three spontaneous mutants (Fig. 3.1). In

addition, these three spontaneous mutants, S1, S2 and S3 can grow faster than previous discovered multi-copy suppressors, such as *MSS51*, *ATP1*. S1 strain needs 3 days to become visible on the YPLG plate while the strains overexpressing *MSS51*, *ATP1* need 6 days. These three spontaneous mutants grow as well like WT (Fig. 3.2A). The known suppressors of coa1∆ were sequenced by a traditional PCR amplification strategy to guarantee we did not isolate a previously identified suppressor. After confirmation of no known mutations S1 strain was dissected to four spores A1, A2, A3 and A4. The growth test suggests A2 and A4 have the suppressing mutation of *coa1Δ* inherited from S1, but A1 and A3 do not have (Fig.3.2B).

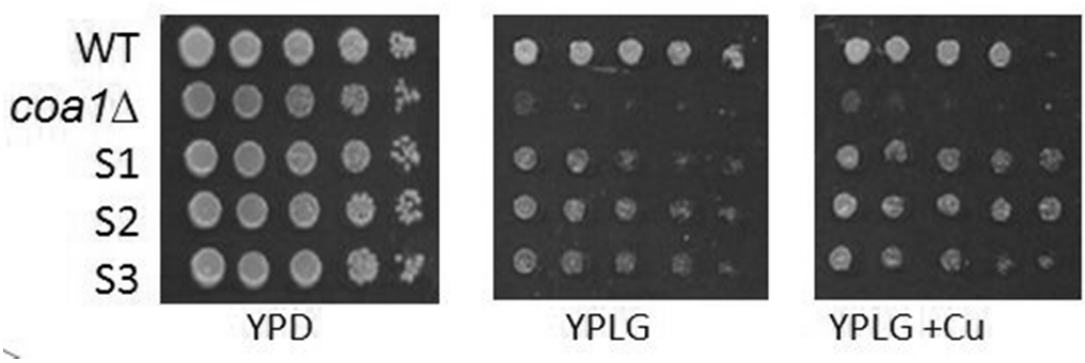

Figure 3.1 Spontaneous mutants S1, S2, S3 in *coa1Δ* were isolated. WT, *coa1Δ*, S1, S2 and S3 cells were grown in SC-2% glucose, serially diluted and spotted on SC-2% glucose, SC-2% glycerol and SC-2% glycerol plus copper medium. The plate were incubated at 30℃for phenotypes.

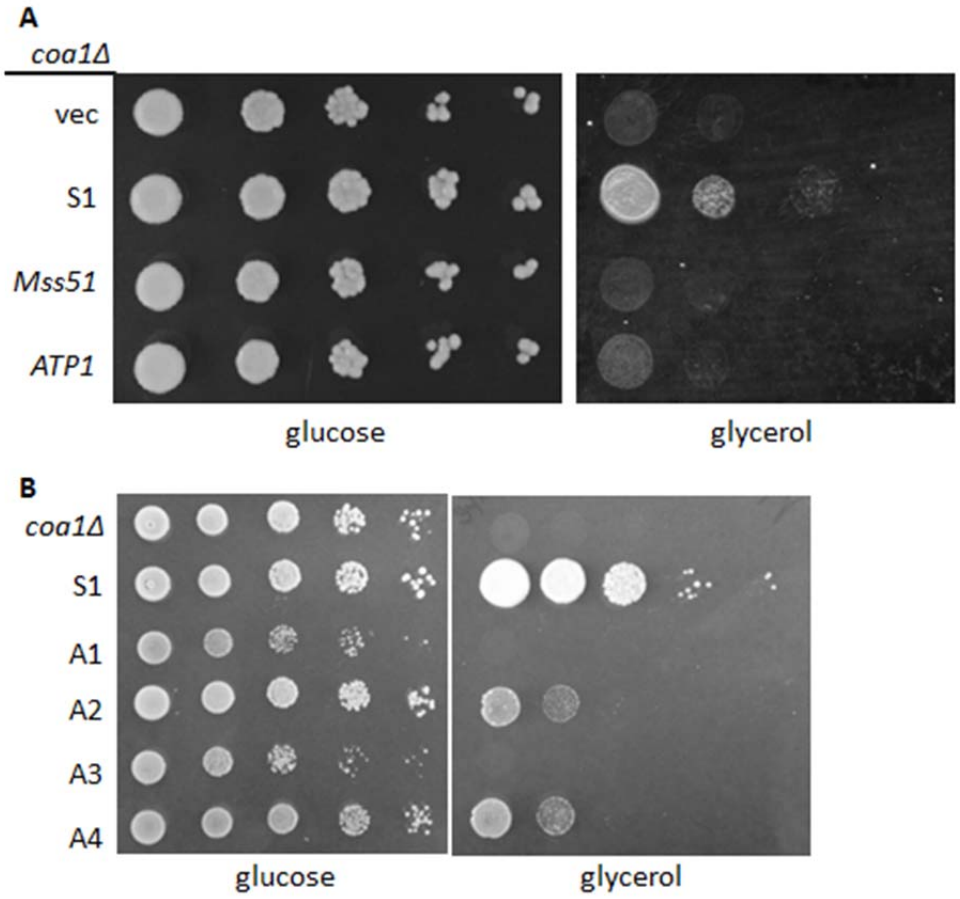

Figure 3.2 (A) *coa1Δ* cells with empty vector (vec) or suppressor MSS51, *ATP1* and its spontaneous mutant S1 were grown in SC-2% glucose with selection, serially diluted and spotted on SC-2% glucose, SC-2% glycerol medium. (B) *coa1Δ*, S1, A1, A2, A3 and A4 cells were grown SC-2% glucose, serially diluted and spotted on SC-2% glucose, SC-2% glycerol medium.

Initial process of the high-throughput sequencing data

Four sequencing DNA libraries were prepared from haploid strains, A1, A2, A3 and A4. The sequencing DNA libraries were pooled, denatured and sequenced on illumina MiSeq sequencer. In total, 4.1G data were produced. The sequencing data quality is very good, with 92.4% data have a Quality Score (Q-score) above 30 and the cluster passing filter (CPF) is 89.8%. A Q-score is a prediction of the probability of a wrong base call. The Q-score above 40 (Q40) means the probability of wrong base call is 1 in 10,000 and Q30 indicates the probability of wrong base call is 1 in 1,000. The CPF shows the percentage of clusters passing filter based on the Illumina chastity filter, which measures quality. The chastity of a base call is the ratio of the intensity of the greatest signal divided by the sum of the two greatest signals. Reads do not pass the quality filter if more than one base call has a chastity value of less than 0.6 in the first 25 cycles.

The high-throughput sequencing data was imported into CLC genomic workbench software. The whole genome of *Saccharomyces cerevisiae* S288C, including 16 chromosomes and one mitochondrial chromosome (NCBI database) were used as a reference. Initially, the sequencing data was trimmed, mapped to each chromosome reference separately using default settings of the software. According to the growth test of A2 and A4 were considered to have the mutation which can suppress the respiration deficiency of *coa1Δ*. The mapping results of A2 and A4 were merged together for single

nucleotide polymorphism (SNP) detection. The A1 and A3 mapping results were compared to S288c for SNP detection separately. The standard code and mitochondria code were used for nuclear genome SNP detection and mitochondrial SNP detection. Finally, the SNPs detected from the merged mapping result of A2 and A4 were pooled with SNPs from A1 mapping result and A3 mapping result to screen those SNPs that only present in A2 and A4 and not exist in A1 or A3. In order to figure out the target mutation from the sequencing data, we set up criteria for screening the SNP: 1. the minimum coverage at the SNP position is four; 2. the minimum variant frequency is 70%; 3. the SNP should only present in A2 and A4; 4. the SNP is not in a transposon/telomere region; 5. The SNP should change an amino acid or at upstream region of some gene (affect promoter); 6. The affected ORF is a mitochondrial related protein.

Initial SNP candidates

The SNP candidate list using the above criteria included many SNPs located in the transposon, telomere region and many serial SNPs found in one gene. Most of the alleles have a variant frequency > 70% but far below 95%, which suggests possible false positive SNP. In addition, except for MKK1, all of them do not exist in parent strain background BY4743 (combined BY4741 and BY4742) when compared to the reference strain S288C. Many of the SNP candidates belong to highly repeated gene family, like *FLO*, *COS*, *HXT*, *PAU*.

Validation of sequencing data

To validate the sequence we created a mapping report that suggests some gaps exist. After analyzing the gap sequence on using BLAST, we found are deleted sequences matched the amino acid gene mutated for auxotrophic selection and the *COA1* gene. Additionally, we identified a 144 bp of *ATP2* gene in A1 and A3. The distribution of these deletions in A1, A2, A3 and A4 is consistent with the 2:2 segregation of alleles from the S1 homozygous yeast cell (Table 3.1). The growth test of A1, A2, A3 and A4 on plates lacking specific amino acid plate is consistent with the deletion distribution of amino acid gene on A1, A2, A3 and A4 (Fig.3.3).

In addition to the amino acid synthesis gene, we also identified known SNP from BY4741 and BY4742 background compared to S288C, demonstrating that quality of the sequencing data. For example, we observed a 2:2 segregation of a SNP (G→C) at 664 nucleotide position of *MKK1* in A2 and A4 sequence consistent with the known Cytosine in BY4741 reference sequence and Guanine in BY4742 reference sequence. In A1 and A3 sequence, we found there is a SNP in YGL260W gene, which is not present in A2 and A4 (Table 3.3) (Fig.3.4).

Table 3.1 Distribution of gene deletions in the four haploid genomes[1]

	A1	A2	A3	A4
chr2	*LYS2*			*LYS2*
Chr3	*LEU2*	*LEU2*	*LEU2*	*LEU2*
chr5	*URA3*	*URA3*	*URA3*	*URA3*
chr9	*COA1*	*COA1*	*COA1*	*COA1*
chr10	144bp of *ATP2*		144bp of *ATP2*	
chr12	*MET17*	*MET17*		
chr15	*HIS3*	*HIS3*	*HIS3*	*HIS3*

1. consensus sequence was assembled by CLC genomic workbench; area of coverage =0 identified from the mapping report

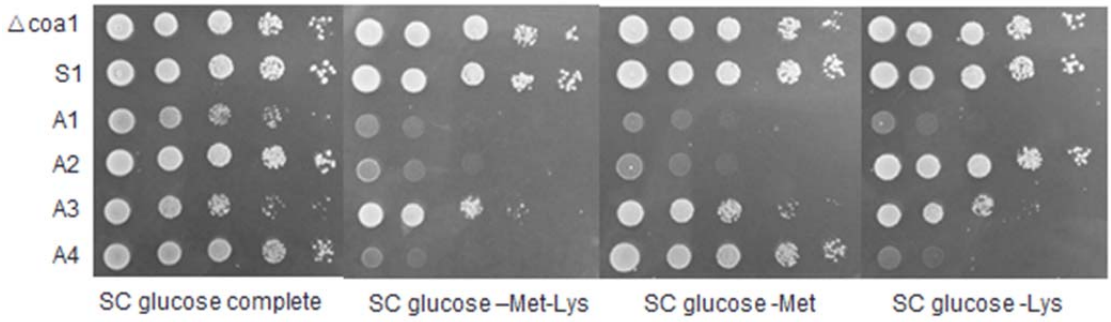

Figure 3.3 Growth tests of A1, A2, A3, and A4. *coa1Δ*, S1, A1, A2, A3 and A4 cells were grown in SC-2% glucose, serially diluted and spotted on SC-2% glucose, SC-2% glucose minus Met and Lys, SC-2% glucose minus Met, SC-2% glucose minus Lys. The plate were incubated at 30℃for phenotypes.

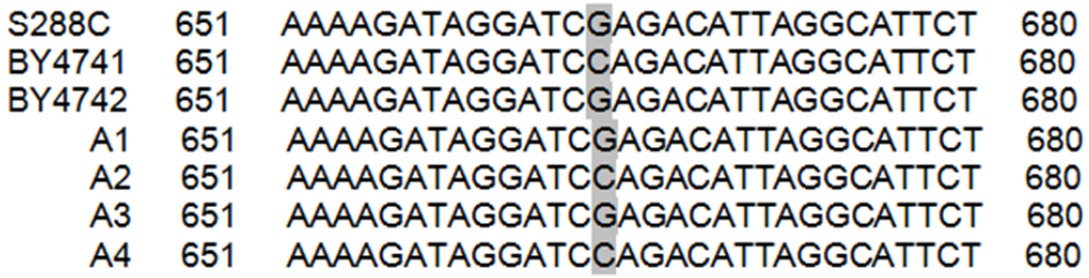

Figure 3.4 *MKK1* SNP only present in A2 and A4; consensus sequence for S288C, BY4741 and BY4742 was retrieved from SGD and the CLC sequence.

Mismatch cause false SNP

Since the sequencing quality is very good there are potential flaws with the screening method or PCR errors. Although it is possible PCR errors can occur during the sequencing reaction, the probability that the error occurs removing the SNP is unlikely due an apparently impossibly low probability.

According to the detailed mapping report, there are many mismatches during the mapping. Although we have excluded the SNPs located in or beside transposon and telomere regions, there are still so many abnormal serial SNP single genes. Even if there are new mutations occurring during growth of they should not be so many serial SNP. Many of these mismatches in highly homologous genes may have resulted from mapping complete sequence whole genome sequence data set to each individual chromosome.

Therefore, sequence was remapped after joining all the chromosomes into one reference sequence. The mapping results of merged A2 and A4 were compared to A1 and A3 mapping results. The position of SNP on the merged reference now needs to be calculated as each chromosome identity is lost in the merge. This strategy showed with merged reference solved the serial false SNP problem and generated a new SNP list (Table 3.3; Table 3.4; Table 3.5). Based on the separately mapping sequencing data to each individual chromosome is we did not reassess the position of deletions in the sequences.

Mapping SNP discovered in BY4743 compared to S288C

The mapping report suggests the whole genome were covered very well with around 99.9% sequence were covered. The maximum coverage in A1, A2, A3 and A4 are from 9389 to 15948. The average coverage in A1, A2, A3 and A4 is from 31.37 to 92.31 (Table 3.2). For the place with zero coverage, many of them are due to gene deletion (Table 3.1)

After fixed the mapping problem, although we set the minimum variant frequency at 70%, however almost all SNP found that only present in A2 and A4 have a variant frequency close to 100%. However, some of them have low coverage, therefore we checked their authenticity of each mutation. After excluding false SNP's due to low coverage place, MKK1 is the only SNP present exclusively in A2 and A4 (Table 3.3) a known SNP present in BY4743 background at 2:2. Since the spontaneous S1 strain is BY4743 *coa1Δ* we did not identify a novel mutation in this background. The analysis of A1 and A3 does identify SNPs only present in A1 and A3 (Table 3.4) and the SNPs present in all four strains, A1, A2, A3 and A4 (Table 3.5).

We wonder whether the reason of not being able to find the suppression mutation in A2 and A4 is the mapping errors in SNP detected by the CLC genomic software, because the trimmed areas and excluded sequences sometimes contain many WT bases exist at the SNP position, but it was called as an SNP by CLC. Therefore, we reanalyzed the sequencing data with the alternative software platform "Geneious" by setting minimum coverage at 1

and MVF at 70%. The other parameters were used the default setting. The analysis result got by Geneious showed us almost the same thing as we found by CLC genomic workbench. Although there are some new SNP discovered and several insertion mutations listed that only exist in A2 and A4, however, except MKK1, most of them locate in telomere region and none of them locate in any ORF or the near upstream region of any ORF (Table 3.6). No deletion mutations were found that only exists in A2 and A4. In addition, although the minimum coverage was set at 1 when using Geneious software, all the variants that only exist in A2 and A4 have coverage above 4. According to this reanalysis, we can say failing to find a unique suppression mutation that only exist in A2 and A4 is not due to software error.

Table 3.2 mapping report[1]

Reference Coverage statistics	**A1**	**A2**	**A3**	**A4**
Total reference length	12157105	12157105	12157105	12157105
Total consensus length	12138198	12144431	12148512	12144704
Fraction of reference covered	0.998444	0.998957	0.999292	0.998979
Minimum coverage	0	0	0	0
Maximum coverage	10488	9389	15948	15623
Average coverage	71.43	31.37	80.39	92.31
Mean read length	244.21	244.49	243.1	241.82
Zero coverage regions				
Count	88	77	62	52
Minimum length	1	1	2	1
Maximum length	4495	2953	2928	4495
Total length	18913	12684	8610	12418

1. Consensus sequence was assembled by CLC genomic workbench; mapping report generated by CLC genomic workbench.

Table 3.3 SNP only in A2 and A4[1]

Reference position	Frequencies	Overlapping Annotations	Amino Acid Change
chromosome 15			
773264	99.1	MKK1	p.Glu222Gln

1. Consensus sequence was assembled by CLC genomic workbench; SNP identified with setting parameter at minimum coverage=4, MVF=70%

Table 3.4 SNP only in A1 and A3[1]

Reference position	Frequencies	Overlapping Annotations	Amino Acid Change
chromosome 2			
5983	98.1	TEL02L	
chromosome 4			
1014995	100	MTH1	
chromosome 7			
6461	100	PAU11	
6476	100	PAU11	
6799	100		
6822	100		
6857	100		
6904	100	YGL260W	
6905	100	YGL260W	p.Leu16Phe
6925	100	YGL260W	

1. Consensus sequence was assembled by CLC genomic workbench; SNP identified with setting parameter at minimum coverage=4, MVF=70%

Table 3.5 SNP in all the four strain A1, A2, A3 and A4[1]

Reference position	Frequencies	Overlapping Annotations	Amino Acid Change
chromosome 1			
25340	100	FLO9	p.Ala877Ser
25488	98.2	FLO9	
25497	100	FLO9	
25506	98.1	FLO9	
25509	99	FLO9	
25512	97.9	FLO9	
25515	96.8	FLO9	
25536	98.8	FLO9	
25542	98.8	FLO9	
25560	95.4	FLO9	
25584	98.4	FLO9	
25611	75	FLO9	
25872	100	FLO9	p.Ile699Met
26058	95.2	FLO9	p.Ile637Met
26412	100	FLO9	p.Ile519Met
26900	100	FLO9	p.Ile357Val
26901	100	FLO9	
26923	100	FLO9	p.Arg349Pro
26931	88.5	FLO9	
26946	70.7	FLO9	
26973	100	FLO9	
26979	94.5	FLO9	
26981	99.2	FLO9	p.Ser330Gly
26982	91.7	FLO9	
26983	100	FLO9	p.Asn329Thr
27027	100	FLO9	
27035	100	FLO9	p.Ile312Val
27036	100	FLO9	
27044	97.9	FLO9	p.Val309Ile
27060	96.7	FLO9	
27063	99.4	FLO9	
27072	91	FLO9	
27075	93.3	FLO9	
27081	95.9	FLO9	
27084	97.3	FLO9	
27126	85.7	FLO9	
27129	93.1	FLO9	
41475	100	GPB2	

141030	100	SSA1	
141135	100	SSA1	
199811	100		
206126	100	FLO1	
206129	98.3	FLO1	
206132	99.2	FLO1	
206144	98.3	FLO1	
210818	100		
211019	100		
chromosome 2			
6440	100	TEL02L	
7510	100		
7511	100		
15101	100	PKC1	p.Ile866Leu
15510	100	PKC1	
15518	100	PKC1	
16380	100	PKC1	
16392	100	PKC1	
30012	100	YBLWTy2-1	
30050	100	YBLWTy2-1	p.Asn39Ser
30658	100	YBLWTy2-1	p.Ala242Ser
30660	100	YBLWTy2-1	
30848	100	YBLWTy2-1	p.Ala305Gly
34298	100	YBLWTy2-1	p.Glu1455Lys
35485	100	YBLWTy2-1	
59755	100		
259764	94.1	YBRWTy1-2	
263153	99	YBRWTy1-2	p.Ser1095Phe
265382	98.6	YBRWTy1-2	
389428	100	ARS213	
389429	83.3	ARS213	
389430	100	ARS213	
chromosome 3			
84421	100	Ty1 LTR	
84780	100		
143131	100		
148615	100	SRD1	p.Glu97Lys
162361	100		
162396	100		
162640	100	hypothetical protein	p.Ser76Arg
162694	100	hypothetical protein	
163059	98.9	PMP1	
199081	98.6	BUD5	

chromosome 4			
757631	95.5	NUM1	
758310	100	NUM1	p.Ser895Pro
783598	100	SEC1	
864219	100	EBS1	
880697	97.3	YDRCTy1-2	p.Val1077Ala
987244	95	YDRCTy1-3	
1253397	100	SAC7	
1308011	88.2	HKR1	p.Val582Ala
1308047	100	HKR1	p.Val594Ala
1402305	100	RPL27B	p.Ser51Leu
1433710	100	PKH1	p.Phe187Ile
1524974	100	TEL04R	
1525313	100	TEL04R	
1525335	100	TEL04R	
1525340	100	TEL04R	
1525345	100	TEL04R	
1525351	100	TEL04R	
1525357	100	TEL04R	
1525363	100	TEL04R	
1525370	100	TEL04R	
chromosome 5			
48384	100		
154531	100	MNN1	p.Ser338Thr
352394	100	SHC1	p.Lys233Glu
517529	100		
chromosome 7			
386978	100	PYC1	p.Arg595Gly
386979	100	PYC1	p.Arg595Pro
401674	100	Ty3 LTR	
401698	100	Ty3 LTR	
404935	100		
404936	100		
chromosome 8			
216123	100	RSC30	p.Gly571Asp
417054	100	KEL1	
499958	100	PPX1	p.Glu396Lys
511255	99	SCH9	
524447	100		
chromosome 9			
318694	100	VID28	p.Asn758Tyr
chromosome 10			
97478	100		

199170	100	hypothetical protein	
200219	100	hypothetical protein	p.Tyr514Cys
525782	86.5		
715095	89.1	DAN4	p.Pro216Ser
715099	81	DAN4	
715108	76.7	DAN4	
715114	83.5	DAN4	
715122	78.8	DAN4	p.Pro207Ser
715126	73.6	DAN4	
715129	86.5	DAN4	
715132	82.1	DAN4	
740238	100		
745747	91.7	TEL10R	
chromosome 11			
666557	100	TEL11R	
chromosome 12			
4	96.1	TEL12L	
12	72.3	TEL12L	
291384	100	GAL2	
291386	100	GAL2	p.His392Arg
468701	100	rRNA	
528749	100	MDL1	p.Phe150Leu
725936	100		
828903	100	ORM2	
944238	98.8	YLRWTy2-1	p.Gln919Lys
1039435	100	SST2	p.Glu644Asp
chromosome 13			
34473	100	NAB6	p.Phe77Leu
325905	100	hypothetical protein	p.Ile10Asn
361550	100	YMRCTy1-3	p.His360Tyr
448333	100		
448334	100		
630505	100	hypothetical protein	p.Asp494Gly
672129	100	PFK2	p.Lys880Glu
680936	98.9	HFA1	p.Lys877Glu
680940	100	HFA1	
809198	100	Ty1 LTR	
908185	81.6	hypothetical protein	
908196	89.6	hypothetical protein	p.Trp278Ser
908198	88	hypothetical protein	p.Ala279Ser
908203	85.1	hypothetical protein	
908218	88.8	hypothetical protein	
924341	87.2	TEL13R	

chromosome 14			
189585	100	SLA2	p.Ser512Phe
377887	100	KRE33	p.Gly856Val
415071	88.9	DBP2	
415088	77.8	DBP2	
415096	87	DBP2	
471767	100	SAL1	p.Met131Val
chromosome 15			
50002	100	CTR9	
50010	100	CTR9	p.Trp927Arg
50012	100	CTR9	p.Gly926Glu
60240	100		
79297	100	YGK3	
79304	100	YGK3	p.Ile59Asn
79305	100	YGK3	p.Ile59Phe
chromosome 16			
191944	100	POS5	p.Ser180Leu
759400	100	RRG8	p.Asn251Lys
890346	100	DPB2	p.Phe458Tyr
mito-chromosome			
16443	100	COX1	p.Val60Leu
20934	100	COX1	p.Ser224Ala
33743	100		
39517	100	COB	p.Gly269Val
82507	100		

1. Consensus sequence was assembled by CLC genomic workbench; SNP identified with setting parameter at minimum coverage=4, MVF=70%

Table 3.6 SNP only in A2 and A4 identified by the “Geneious” platform.[1]

Reference position	Variant Frequency	Overlapping Annotations	Polymorphism Type
chromosome1			
23737	78%		Insertion (tandem repeat)
chromosome3			
316619	93%	telomere	SNP
chromosome4			
126566	88%	VMA1 upstream221bp	Insertion (tandem repeat)
678049	100%		SNP
chromosome13			
25	96%	telomere	Insertion (tandem repeat)
924385	96%	telomere	SNP
924390	100%	telomere	SNP
924392	100%	telomere	SNP
chromosome14			
784322	73%	telomere	SNP
chromosome15			
773264	100%	MKK1	SNP
chromosome16			
948065	100%	telomere	SNP

1. Consensus sequence was assembled by Geneious; SNP identified with setting parameter at minimum coverage=1, MVF=70%

Validating mutations

Possible reasons for not identifying a nuclear mutation responsible for the suppression are 1. An error caused by mapping mismatch make the SNP has a variant frequency lower than the MVF (70%). However, in this case, the frequency of WT would exceed 30%, which is very unlikely; 2. The mutation is located in gap or in excluded region, such as transposon or telomere region; 3. There might be several alleles that work together; 4. It is some epigenetic modification in A2 and A4 which can also segregate 2:2.

Initially we expected a single mutation that only present in A2 and A4 that acted as a dominant suppressor of the respiration deficiency of *coa1Δ.* However given the quality of the sequencing we considered the possibility that the SNP in gene YGL260W, present in A1 and A3 only, could be responsible for the growth defect of the original *coa1*Δ that is reverted in S1 to allow growth on respiratory medium (Table 3.4) (Fig.3.5). Overexpressing YGL260W from A2 in A1 did not improve the growth of A1 on glucose and glycerol medium (Figure 3. 6).

ATP2 is partially deleted in A1 and A3 (Fig.3.7). PCR product of *ATP2* in *coa1Δ*, S1, A1 and A2 showed that *ATP2* is complete in *coa1Δ* and A2, partial deleted in A1. In S1, both the complete and the partial deleted *ATP2* exist suggesting it is heterozygous (Fig.3.8A). Since A1 and A3 do not grow well on glucose medium, especially YPD plate (Fig.3.8B), we tested whether it is

because A1 and A3 have *ATP2* partial deletion. As for *ATP2* deletion, although *coa1*Δ or *atp2*Δ single deletion both can grow well on glucose plate (Fig.3.1) (Fig.3.8C), we still transformed and overexpressed *ATP2* gene from A2 into A1. The growth of A1 on glucose plate was rescued (Fig.3.8D), which suggests that *coa1*Δ or *atp2*Δ have synthetic defect. Considering the growth defect of A1 and A3 on glucose plate caused by the partial deletion of *ATP2*, we tested whether the glycerol growth defect of A1 and A3 could be reversed by *ATP2*. The growth test suggests that overexpressing *ATP2* gene from A2 into A1 or A3, the growth defect on glycerol was suppressed. This means the suppression mutation in S1 separated into all the four haploid strain (A1, A2, A3 and A4). The reason that A1 and A3 cannot grow on glycerol is due to the *ATP2* deletion. Given the frequency of isolation of 1 3.8 x10^6 and that it exists in all the four haploid strains is the one that suppresses the glycerol growth defect we focused on mitochondrial mutations. As the likelihood that the mutation occurs on both chromosomes in S1 is very low. And at the same time, we found a novel mitochondrial SNP that exist in COX1 (Fig.3.9). This COX1 SNP only exists in S1 and not in the original *coa1*Δ strain background (Fig. 3.10). We took this novel COX1 SNP as a candidate for the suppressing mutation. To verify whether this unique COX1 SNP is the mutation that suppresses the glycerol growth defect we removed the mitochondrial genome of the haploid strain A2, A4 and *coa1*Δ to produce haploid A2 ρ cell, A4 ρ cell and *coa1*Δ ρ cell. Then, we crossed “A2 ρ cell with *coa1*Δ cell”, “A4 ρ cell with

*coa1*Δ cell", "A1 cell with *coa1*Δ ρ cell" and "A3 cell with *coa1*Δ ρ cell" to produce diploid cells. If the novel COX1 SNP is the suppression mutation, the diploid cell "A2 ρ + *coa1*Δ" and "A4 ρ + *coa1*Δ" should be unable to grow on glycerol plate because they don't have the novel COX1 SNP mutation. The diploid cell "A1 + *coa1*Δ ρ" and "A3 + *coa1*Δ ρ" should also be able to grow on glycerol plate because the presence of the novel COX1 SNP.

As for the A2 and A4 haploid strain, although they are able to grow on glycerol medium, however, they grow much weaker than S1 (Fig. 3.11A). This suggests that although A2 and A4 contain the suppression mutation, but still lack something. Since there is an *ATP2* partial deletion mutation and considering the *ATP1* multi-copy suppressor we discovered in Chapter 2, we hypothesize that the *ATP2* deletion in A1 and A3 may have something to do with the growth. We mate A2 ρ cell with A1 cell and did growth test. The new generated diploid cell "A2 ρ + A1" grows as well as S1 strain on glycerol plate (Fig.3.11B), which suggests there must be something in A1 that enhance the growth of A2 on glycerol. We wonder whether it's the deletion of *ATP2* that enhance the growth of A2. In ATP synthase, *ATP1* encodes the alpha subunit and *ATP2* encodes the beta subunit. In one ATP synthase, there are three pair of alpha and beta subunits associating together to function producing ATP. Because overexpressing *ATP1* could suppress *coa1*Δ, we wonder whether the deletion of *ATP2* has the similar effect since there are extra *ATP1* that cannot pair with *ATP2*. We transformed *ATP2* in S1 strain and detected the oxygen

consumption to see whether overexpressing *ATP2* can affect the growth of S1. The result suggests that overexpressing of *ATP2* in S1 decreased the oxygen consumption of the S1 cell (Fig.3.11C).

In conclusion，based on the superior growth of S1 compared to A2 or A4, we suggest that the heterozygous *ATP2* allele improves growth by increasing the apparent copy number of *ATP1*. However, we hypothesize that glycerol growth is dependent on the unique *COX1* allele. Further analysis will be required to verify this hypothesis.

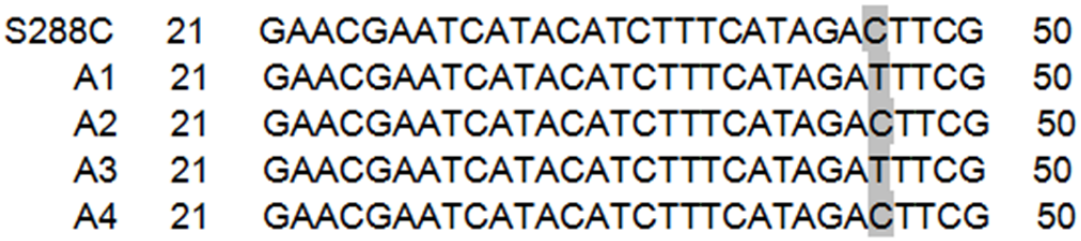

Figure 3.5 YGL260W SNP only present in A1 and A3

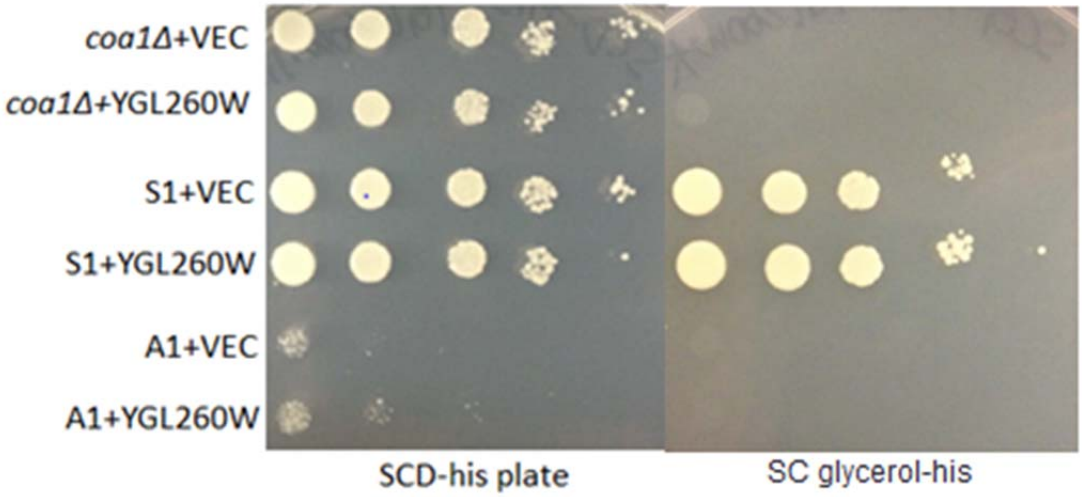

Figure 3.6 YGL260W from A2 cannot rescue A1 growth deficiency on glucose and glycerol medium

(The 1001st bp position of *ATP2*)→
AGGGTTCTGTCACTTCTGTGCAAGCCGTTTATGTTCCAGCCGATGATTTAACAGATCCTGCTC
CTGCCACTACTTTTGCCCATTTGGACGCTACTACCGTCTTGTCAAGAGGTATTTCAGAATTAG
GTATTTACCCTGCAGTGGATCCATTGGATTCTAAATCAAGGTTATTGGATGCCGCCGTTGTCG
GTCAAGAACATTATGACGTCGCCTCCAAGGTTCAAGAAACTTTACAGACCTATAAATCTTTACA
AGATATCATTGCTATTTTGGGTATGGATGAATTGTCCGAACAAGATAAACTAACTGTCGAAAG
GGCAAGAAAGATTCAAAGATTCTTATCTCAACCATTTGCTGTCGCCGAAGTCTTTACTGGTAT
CCCAGGTAAATTAGTGAGATTAAAGGACACCGTTGCCTCGTTCAAAGCCGTTTTGGAAGGTAA
ATACGATAATATACCAGAACATGCTTTCTATATGGTTGGTGGTATTGAAGATGTTGTTGCTAAA
GCTGAAAAGTTAGCCGCTGAAGCCAACTAG ←(The end of *ATP2*)

Figure 3.7 The gray sequence in *ATP2* was deleted in A1 and A3

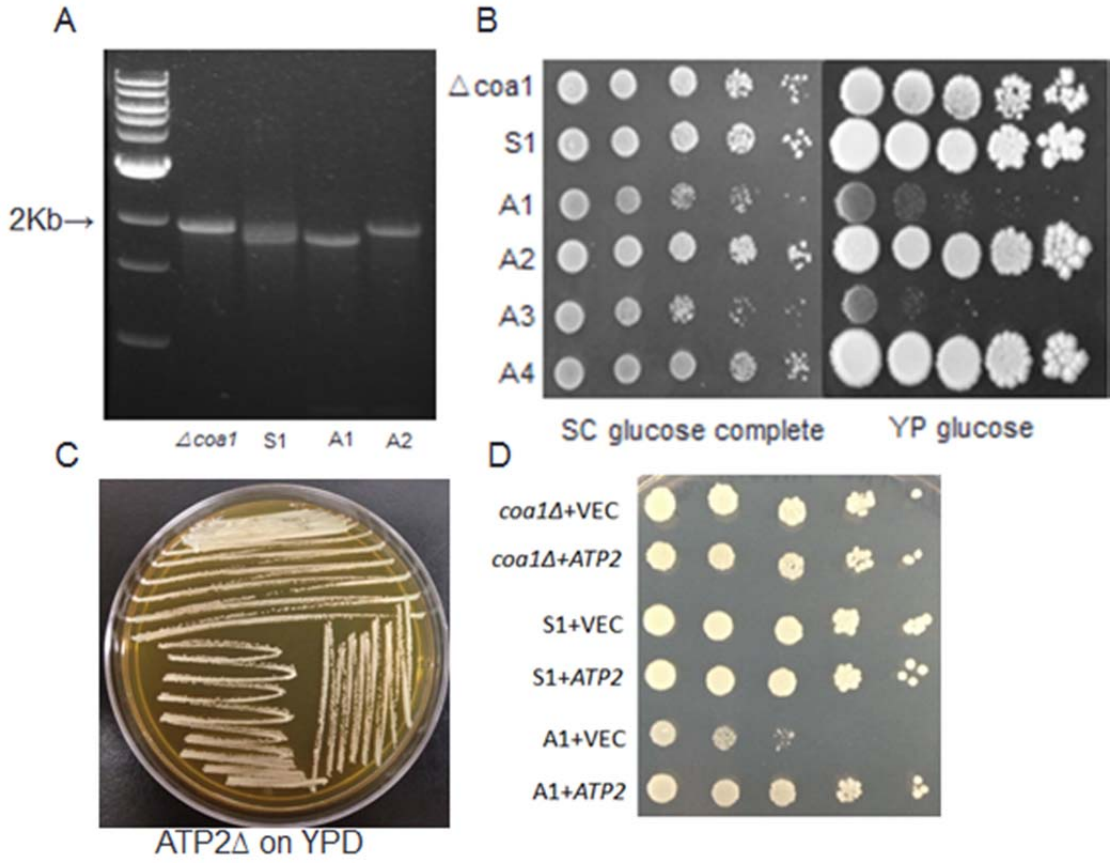

Figure 3.8 (A) PCR product of *ATP2* gene from *coa1Δ*, S1, A1 and A3 were run on agarose gel. (B) *coa1Δ*, S1, A1, A2, A3 and A4 cells were grown in SC-2% glucose, serially diluted and spotted on SC-2% glucose and YP glucose plates. The plate were incubated at 30℃ for phenotypes. (C)*ATP2* Δ grows well on glucose medium. (D) *ATP2* from A2 can rescue A1 growth deficiency on glucose plate.

Reference position	Frequencies	Overlapping Annotations	Amino Acid Change	
mito-chromosome				
16443	100	COX1	p.Val60Leu	Unknown
20934	100	COX1	p.Ser224Ala	Known
33743	100			
39517	100	COB	p.Gly269Val	
82507	100			

1. Consensus sequence was assembled by CLC genomic workbench; SNP identified with setting parameter at minimum coverage=4, MVF=70%

Figure 3.9 Mitochondrial SNP in all the four strain A1, A2, A3 and A4[1]

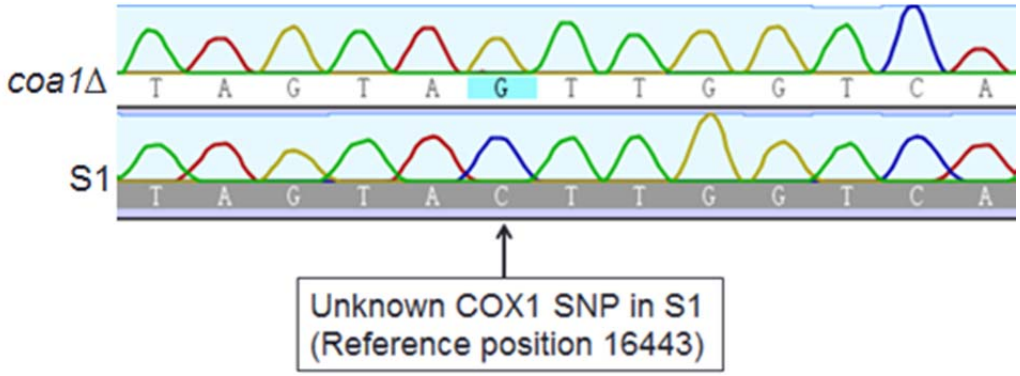

Figure 3.10 The unknown COX1 SNP (Reference position 16443) does not exist in *coa1*Δ (BY4743 strain background)

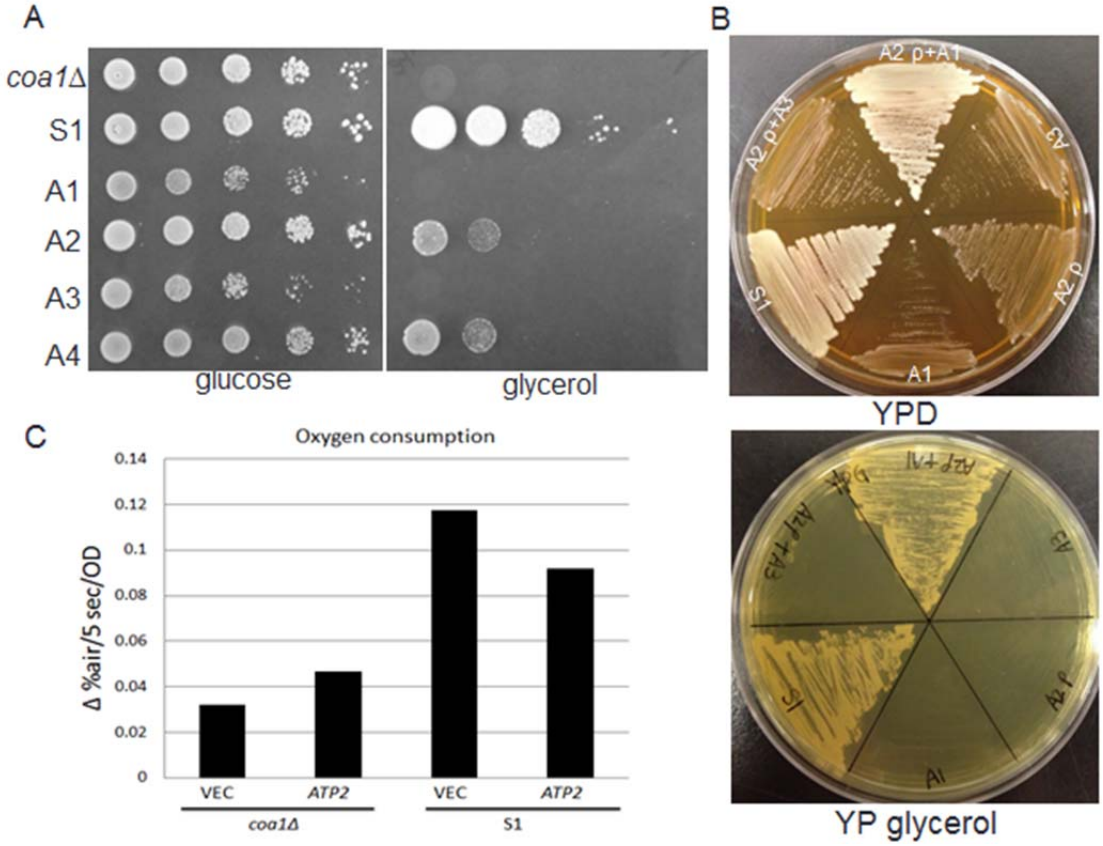

Figure 3.11 (A) A2 and A4 grow much weaker than S1. (B) The new generated diploid cell "A2 ρ + A1" grows as well as S1 strain on glycerol plate. (C) Overexpressing of *ATP2* in S1 decreased the oxygen consumption

6. Reference

[1] C. Honisch, A. Raghunathan, C. R. Cantor, B. Ø. Palsson, and D. van den Boom, “High-throughput mutation detection underlying adaptive evolution of Escherichia coli-K12.,” *Genome Res.*, vol. 14, no. 12, pp. 2495–502, Dec. 2004.

[2] G. J. Velicer, G. Raddatz, H. Keller, S. Deiss, C. Lanz, I. Dinkelacker, and S. C. Schuster, “Comprehensive mutation identification in an evolved bacterial cooperator and its cheating ancestor.,” *Proc. Natl. Acad. Sci. U. S. A.*, vol. 103, no. 21, pp. 8107–12, May 2006.

[3] D. R. Smith, A. R. Quinlan, H. E. Peckham, K. Makowsky, W. Tao, B. Woolf, L. Shen, W. F. Donahue, N. Tusneem, M. P. Stromberg, D. A. Stewart, L. Zhang, S. S. Ranade, J. B. Warner, C. C. Lee, B. E. Coleman, Z. Zhang, S. F. McLaughlin, J. A. Malek, J. M. Sorenson, A. P. Blanchard, J. Chapman, D. Hillman, F. Chen, D. S. Rokhsar, K. J. McKernan, T. W. Jeffries, G. T. Marth, and P. M. Richardson, “Rapid whole-genome mutational profiling using next-generation sequencing technologies.,” *Genome Res.*, vol. 18, no. 10, pp. 1638–42, Oct. 2008.

[4] J. Klockgether, A. Munder, J. Neugebauer, C. F. Davenport, F. Stanke, K. D. Larbig, S. Heeb, U. Schöck, T. M. Pohl, L. Wiehlmann, and B. Tümmler, “Genome diversity of Pseudomonas aeruginosa PAO1 laboratory strains.,” *J. Bacteriol.*, vol. 192, no. 4, pp. 1113–21, Feb. 2010.

[5] D.-H. Lee and B. Ø. Palsson, “Adaptive evolution of Escherichia coli K-12 MG1655 during growth on a Nonnative carbon source, L-1,2-propanediol.,” *Appl. Environ. Microbiol.*, vol. 76, no. 13, pp. 4158–68, Jul. 2010.

[6] P. E. Chen, K. M. Willner, A. Butani, S. Dorsey, M. George, A. Stewart, S. M. Lentz, C. E. Cook, A. Akmal, L. B. Price, P. S. Keim, A. Mateczun, T. N. Brahmbhatt, K. A. Bishop-Lilly, M. E. Zwick, T. D. Read, and S. Sozhamannan, “Rapid identification of genetic modifications in Bacillus anthracis using whole genome draft sequences generated by 454 pyrosequencing.,” *PLoS One*, vol. 5, no. 8, p. e12397, Jan. 2010.

[7] C. D. Herring, A. Raghunathan, C. Honisch, T. Patel, M. K. Applebee, A. R. Joyce, T. J. Albert, F. R. Blattner, D. van den Boom, C. R. Cantor, and B. Ø. Palsson, “Comparative genome sequencing of Escherichia coli allows observation of bacterial evolution on a laboratory timescale.,” *Nat. Genet.*, vol. 38, no. 12, pp. 1406–12, Dec. 2006.

[8] T. M. Conrad, A. R. Joyce, M. K. Applebee, C. L. Barrett, B. Xie, Y. Gao, and B. Ø. Palsson, “Whole-genome resequencing of Escherichia coli K-12 MG1655 undergoing short-term laboratory evolution in lactate minimal media reveals flexible selection of adaptive mutations.,” *Genome Biol.*, vol. 10, no. 10, p. R118, Jan. 2009.

[9] A. Srivatsan, Y. Han, J. Peng, A. K. Tehranchi, R. Gibbs, J. D. Wang, and R. Chen, “High-precision, whole-genome sequencing of laboratory strains facilitates genetic studies.,” *PLoS Genet.*, vol. 4, no. 8, p. e1000139, Jan. 2008.

[10] M. A. Harper, Z. Chen, T. Toy, I. M. P. Machado, S. F. Nelson, J. C. Liao, and C. J. Lee, “Phenotype sequencing: identifying the genes that cause a phenotype directly from pooled sequencing of independent mutants.,” *PLoS One*, vol. 6, no. 2, p. e16517, Jan. 2011.

Chapter 4

Hydroxyurea sensitivity in iron deficient yeast mutants

1. Abstract:

To understand intracellular iron handling, we attempted to use a genetic strategy exploiting the hydroxyurea sensitivity of an iron deficiency (*aft1⊿aft2⊿*) to find component of the pathway. We isolated 6 suppressor mutants of *aft1⊿aft2⊿* double mutant that can tolerate HU and attempted to characterize the suppressing mutation. We screened a HU sensitive revertant (YZ4) using a genomic library from a resistant mutant (YZ2). We note that iron was unable to rescue the HU sensitivity of YZ4 growth deficiency on HU plate suggesting an additional mutation that could reveal an unknown HU sensitive gene. Our genomic library showed *SPT3* was able to rescue the HU sensitivity of YZ4 and that *SPT3* contained a non-sense mutation (*SPT3-1*) in YZ4. Our result showed that *SPT3* mutation affected total cellular metals. The Fe and Zn level is decreased between YZ2 and YZ4 0.7 and 0.6 respectively while Mg, Mn and K are unchanged. The HU sensitivity phenotype of YZ4 *SPT3-1* is in an *aft1*∆*aft2*∆ background we tested if this phenotype was dependent of *AFT1/AFT2* or was a result of *SPT3* deletion. An independent a *spt3*∆ was sensitive to HU and could be rescued by the *SPT3* but not *SPT3-1* in high or low copy vectors.

2. Introduction

Iron (Fe) is an essential metal in yeast required from ribosome assembly and DNA replication. The intracellular levels of Fe are controlled by transporters at the plasma membrane and in the vacuole. Expression of Fe-requiring proteins and the transporters that modulate available Fe is controlled by Fe-regulated transcription factors Aft1 and Aft2 and by post transcription mechanism including protein and mRNA degradation. While all these mechanism interlock to provide necessary cellular requirements the mechanisms for translocation of Fe to targets in the cytosol are largely unknown.

During DNA synthesis, ribonucleotide reductase (RNR) plays an important role by converting ribonucleotide diphosphates into deoxyribonucleotide diphosphates [1]. This is the only mechanism for the production of deoxyribonucleotides in yeast as they lack any deoxyribonucleotide kinase enzymes. Eukaryotic RNRs are constituted by two large and two small subunits and one small subunit has oxo-diferric center making RNR susceptible to Fe-chelators or low available Fe [2]. In fact it has been suggested in some studies that RNR activity is preferentially more sensitive to this inhibition than other essential Fe-requiring enzymes [3]. Part of the catalytic mechanism of RNR includes formation of a tyrosyl radical in the small subunit hydroxyurea (HU) appears to be able to quench this radical leading a DNA replication arrest [1]. The overexpression or mutation of the small subunit

of RNR can increase cellular resistance to HU. Given the high concentration of HU was required for the inhibition of RNR, it has been suggested RNR might be the only essential target for HU in the cell [4].

Many studies of HU response have been done with *Saccharomyces cerevisiae.* An S-phase check-point response was activated by the inhibition of RNR and dNTP synthesis with HU. This response finally leads to transcriptional activation of RNR genes, the stabilization of stalled replication forks, and the inhibition of cell-cycle progression [5]. Numerous genes that help cell tolerate HU have been identified during the screening of deletion mutants of all non-essential genes [6]. An example of non-essential genes that are required for cellular tolerance to HU is *SNF1* [7].

The iron regulated transcription factors Aft1 and Aft2 are also required for tolerance to HU [8]. The phenotypic analyses of single and double *AFT1* and *AFT2* deletion mutants were performed and no phenotype was observed for the *aft1⊿* or *aft2⊿* single mutants on Fe-replete medium with or without HU. But the *aft1⊿aft2⊿* double mutant was sensitive to HU and could not grow on an iron-deprived synthetic medium [8]. The *aft1*Δ single mutant was also sensitive to HU on these iron-deprived medium, but this sensitivity can be suppressed by adding excess iron [8]. This suggests the *aft1⊿aft2⊿* double mutant has low iron utilization and homeostasis that result in sensitive to HU by affecting RNR activity or loading.

We isolated 6 suppressor mutants of *aft1⊿aft2⊿* double mutant that can

tolerate HU. We observed spontaneous loss of suppression in one of the 6 suppressor and attempted in this chapter to identify and characterize the suppression mutation occurs the *aft1⊿aft2⊿* mutant.

3. Materials and methods

Bacterial strains

NEB 10-beta Competent *Escherichia coli* cells (High Efficiency) were used as the bacterial host for genomic library plasmid. NEB 5-alpha Competent *Escherichia coli* cells (Subcloning Efficiency) were used for general plasmid transformation.

DNA manipulations

The genomic DNA was extracted manually with traditional method and can be purified by some genomic DNA clean kit. For plasmid isolation from E. coli and yeast, a Qiaprep Spin Miniprep Kit was used. For plasmid isolation from yeast, the protocol was modified: after resuspending yeast cells in 250ul kit P1 buffer, add 50-100ul of acid-washed glass beads (Sigma G-8772) and vortex for 5min. Let stand to allow the beads to settle. Transfer supernatant to a fresh 1.5 ml microcentrifuge tube. Then proceed to the 250ul kit P2 buffer step and finish the left isolation steps in the kit protocol for E. coli cells.

Genomic library prepare

The genomic library was prepared as described elsewhere [9]. The plasmid pRS413 was cut with EcoRV and treated with alkaline phosphatase (New England Biolabs). The YZ2 cell genomic DNA was partially digested with EcoRV to give a maximum number of DNA fragments in the 3-10 kb size range. Then run these DNA fragments on an agarose gel, cut the DNA smear range from 3-10kb out of the gel and extract with a gel extraction kit. The genomic DNA fragments extracted and the treated pRS413 vector were ligated with T4 DNA ligase (New England Biolabs) at 14 ℃ overnight. The ligation mixture was used to transform NEB 10-beta Competent *Escherichia coli* cells (High Efficiency) with electroporation method. The transformants were selected on LB plates with ampicillin. Then the transformants were scraped off with liquid LB medium and used to extract the genomic library plasmid with a Qiaprep Spin Miniprep Kit.

The total number of colonies needs to be collected is calculated according to the genomic library construction formula:

$$\mathrm{N} = \frac{\ln(1-p)}{\ln(1-\frac{i}{g})}$$

g = genome size

i = insert size

p = probability that any point in the genome will occur at least once in the library

N = number of clones in the library

The calculation is as following:

The genome size (g) of S. cerevisiae is about 13.5Mb; Because the average gene size of S. cerevisiae is 1.5kb (most genes < 5kb; the longest < 10kb), the genomic DNA was partially digested to average size of 6kb (3kb-10kb). So the insert size (i) =6X10^3; Set the probability that any point in the genome will occur at least once in the library (P) =99%

$$N = \frac{\ln(1-p)}{\ln(1-\frac{i}{g})} = \frac{\ln(1-99\%)}{\ln(1-\frac{6\times10^3}{13.5\times10^6})} = 10359$$

4. Results

Six suppressor mutants of *aft1*Δ*aft2*Δ were isolated that were HU tolerant. These strains were designated YZ1 to YZ6. These strains were backcrossed and determined that the phenotypes were from a single mutation in the laboratory of our collaborator Fabien Pierrel CNRS, Grenoble, France. The final mutants were cultured on glucose plates with 0 mM HU, 150 mM HU, 0 mM HU plus iron, 150 mM HU plus iron added and incubated at 37℃ for four days. YZ1, YZ2, YZ3, YZ5 and YZ6 have HU resistant phenotype, while YZ4 was sensitive to HU (Figure 4.1).

For the initial screen we used a genomic library created from the YZ2, which was HU resistant and YZ4 as a recipient strain for complementation

experiments. First, we optimized the concentration of HU added to the SC glucose plate, under which the cells contain suppressor can form colony after 1 day (YZ2 cells), while the cells sensitive to HU cannot form any colony after 1 day growth (YZ4 cells). We plated diluted culture that contains 100 cells to glucose plate at 37℃ for 1 day to form colonies. We then replica plated to HU at 150mM (Fig. 4.2) After screening out some HU suppression candidates from the genomic library, the candidates plasmid were extracted and transformed into YZ4 to check their suppression function. In this way, the candidates that grow on HU because of some new mutation in their genomic DNA, rather than depend on some plasmid contained, can be excluded.

We expected that if YZ4 was a simple revertant we could identify the suppressor from YZ2. However, we note that iron was unable to rescue the HU sensitivity of YZ4 growth deficiency on HU plate suggesting an additional mutation in addition to the aft1Δaft2Δ induced HU sensitivity was present (Fig. 4.1). We continued predicting that YZ4 could reveal additional information such as unknown HU sensitive gene.

ICP analysis of metal level in YZ2 and YZ4

To confirm that we iron was not playing a role in the suppression of YZ2 we assayed total cellular metals using ICP-OES. Whole cells were grown in synthetic complete media, washed and assayed after acid digestion. The total cellular iron level in YZ2 is less than YZ4, suggesting that YZ4 could contain a

mutation that increases cellular Fe in *aft1*Δ*aft2*Δ background. The Fe and Zn level is decreased between YZ2 and YZ4 0.7 and 0.6 respectively while Mg, Mn and K are unchanged. In combination these experiments suggest that the HU sensitivity of YZ4 is not due to iron shortage (Fig. 4.2)

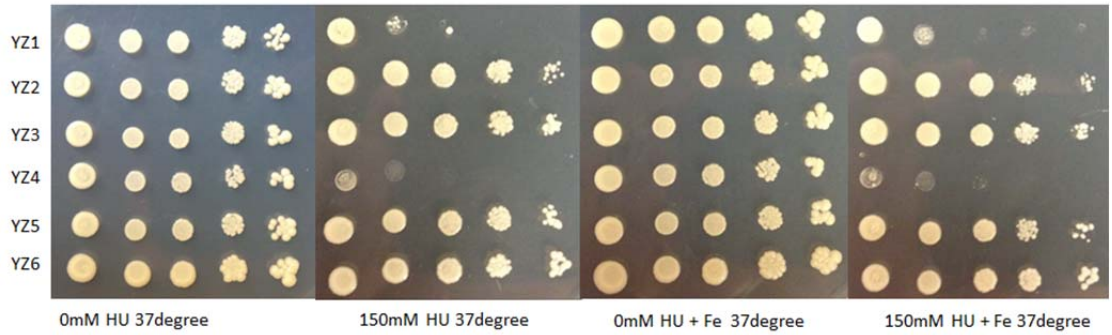

Figure 4.1. Growth test of 6 suppression mutants of *aft1⊿aft2⊿* double mutant on SC glucose plates with 0mM HU, 150mM HU, 0mM HU plus Fe, 150mM HU plus Fe added; incubate at 37℃ for four days.

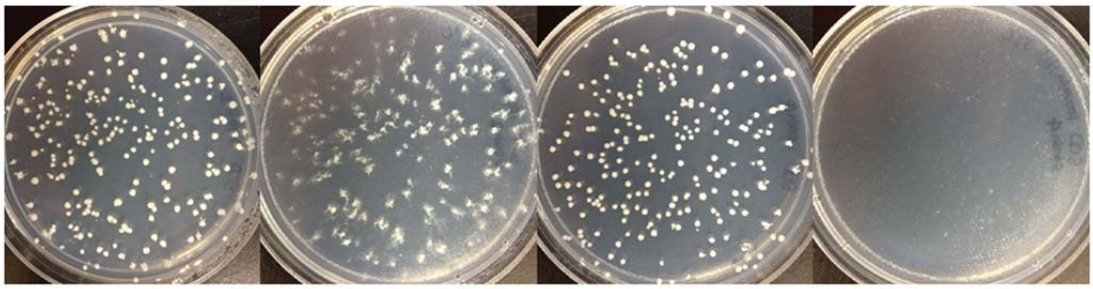

YZ2 100cells SC glucose 37degree 1 day

YZ2 100cells SC glucose 100mMHU 37degree 1 day

YZ4 100cells SC glucose 37degree 1 day

YZ4 100cells SC glucose 100mMHU 37degree 1 day

Figure 4.2. Screen genomic library prepared from YZ2 in YZ4 on SC glucose plus 100mM HU plate at 37℃

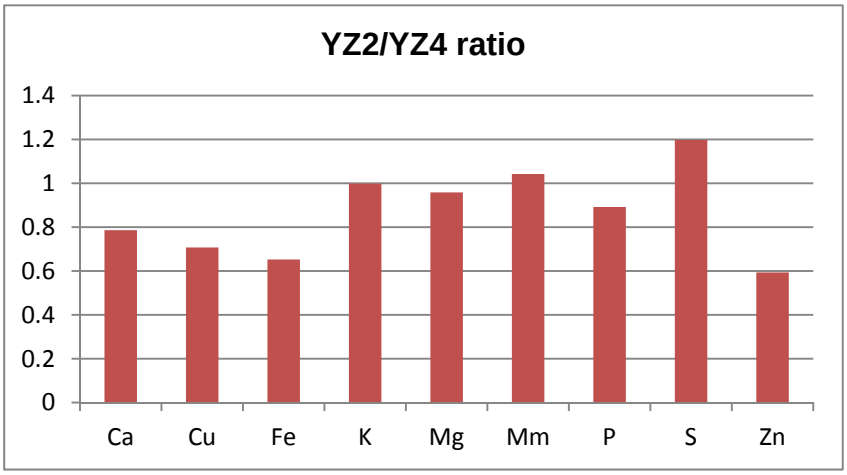

Figure 4.3. YZ2 has less Fe than YZ4, but YZ4 is still sensitive to HU and cannot be suppressed by adding Fe.

Screen genomic library

A genomic library was constructed from YZ2 and was transformed into YZ4 cells to screen for suppressor of the HU sensitivity. From a screen of XXXX candidates we obtained 7 candidates, SUP1 to SUP7. After plasmid rescue and retransformation to ensure linkage to the plasmid SUP1, SUP2, SUP4, SUP6, SUP7 were confirmed as containing the suppressing allele plasmid (Fig. 4.4). All plasmids contained inserts that included *SPT3* gene. *SPT3* was subcloned into high copy plasmid and tested its suppression to YZ4. SPT3 was able to rescue the HU sensitivity of YZ4 in low or high copy vectors (Fig. 4.5)

Alignment of sequencing and translation results of *SPT3* gene in YZ2, YZ4

To investigate the role of *SPT3* in suppression YZ4 on HU sensitivity we considered two possibilities. One is *SPT3* gene from YZ2 has some mutation which make it a suppressor of *aft1⊿aft2⊿* double mutant or *SPT3* gene of YZ4 had a mutation rendering the cells HU sensitive. *SPT3* deletion was not identified as HU sensitive in systematic screens of HU sensitivity. To address these possibilities we amplified and sequenced the *SPT3* gene from YZ2 and YZ4. The sequencing results confirmed a nonsense mutation in *SPT3* gene from YZ4 that we named *spt3-1* (Fig 4.6).

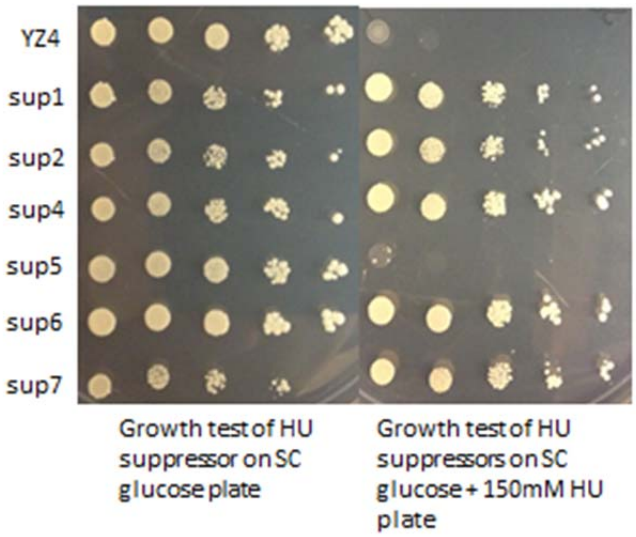

Figure 4.4. Growth test of 6 suppressors identified from genomic library screening on SC glucose plate and SC glucose plus 150mM HU plate.

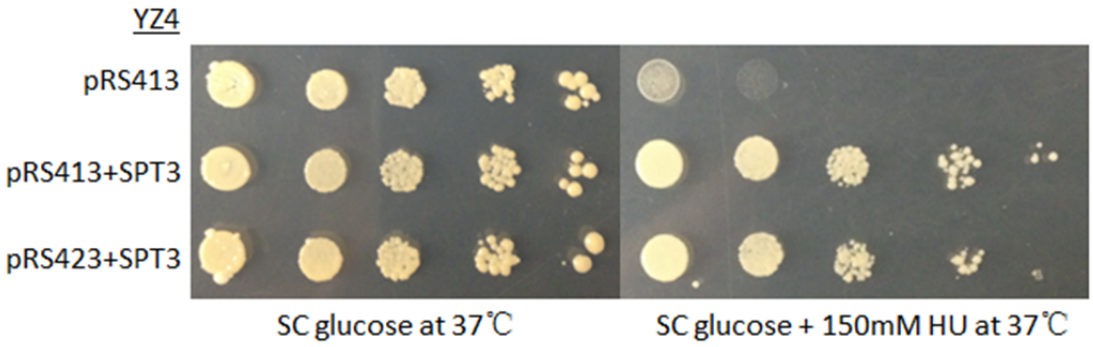

Figure 4.5. Growth test of the HU suppression of YZ4 by *SPT3* in low copy (pRS413) and high copy vector (pRS423)

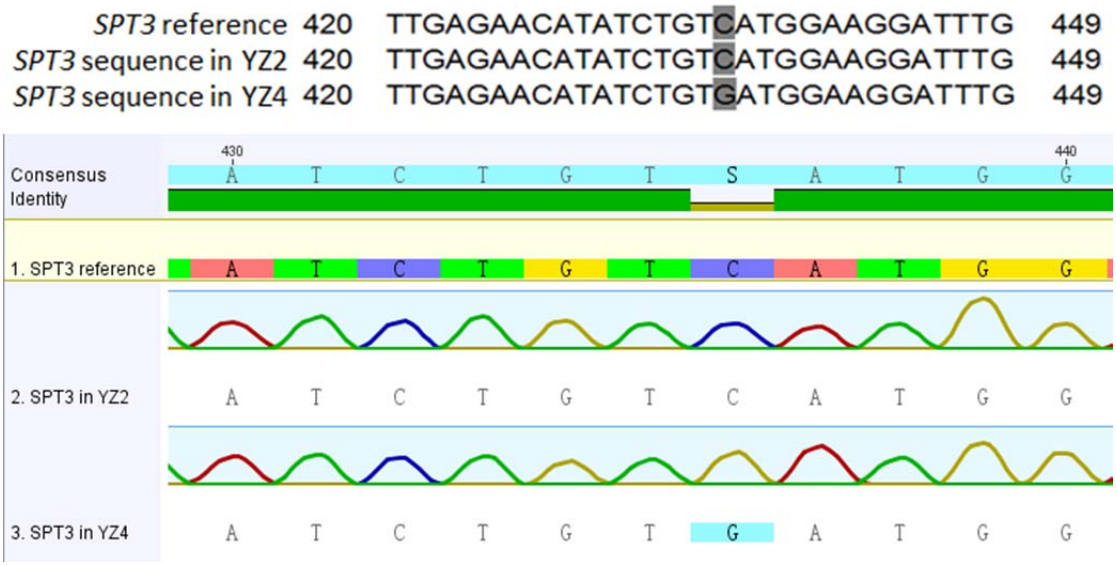

Translation of *SPT3* sequence in reference or YZ2:

MMDKHKYRVEIQQMMFVSGEINDPPVETTSLIEDIVRGQVIEILLQSNKTAHL
RGSRSILPEDVIFLIRHDKAKVNRLRTYLSWKDLRKNAKDQDASAGVASGTG
NPGAGGEDDLKKAGGGEKDEKDGGNMMKVKKSQIKLPWELQFMFNEHPL
ENNDDNDDMDEDEREANIVTLKRLKMADDRTRNMTKEEYVHWSDCRQASF
TFRKNKRFKDWSGISQLTEGKPHDDVIDILGFLTFEIVCSLTETALKIKQREQV
LQTQKDKSQQSSQDNTNFEFASSTLHRKKRLFDGPENVINPLKPRHIEEAW
RVLQTIDMRHRALTNFKGGRLSSKPIIM*

Translation of *SPT3* sequence in YZ4:

MMDKHKYRVEIQQMMFVSGEINDPPVETTSLIEDIVRGQVIEILLQSNKTAHL
RGSRSILPEDVIFLIRHDKAKVNRLRTYL*

Figure 4.6. Alignment of sequencing and translation results; * stands for stop codon

ICP analysis of metal content in "YZ4 complemented by SPT3" versus YZ4

YZ4 had shown increased iron levels relative to YZ2 and to assay for the involvement of *spt3-1* or whether the change in metal content was related to an additional mutation we measured the iron level of YZ4 plus wild-type *SPT3*. The re-introduction of *SPT3* into YZ4 resulted in decreased cell levels of Fe, with *spt3-1*/*SPT3* showing a ratio of 0.4.

Growth test of the HU suppression of YZ4 and BY4741 *spt3Δ*

As the HU sensitivity phenotype of *spt3-1* is in an *aft1*Δ*aft2*Δ background we tested if this phenotype was dependent of *AFT1/AFT2* or was a result of *SPT3* deletion. As noted earlier the SPT3 has not previously been linked with sensitivity and expression of SPT3 did decrease cellular Fe. However a *spt3*Δ was sensitive to HU and could be rescued by the *SPT3* but not *SPT3-1* in high or low copy vectors.

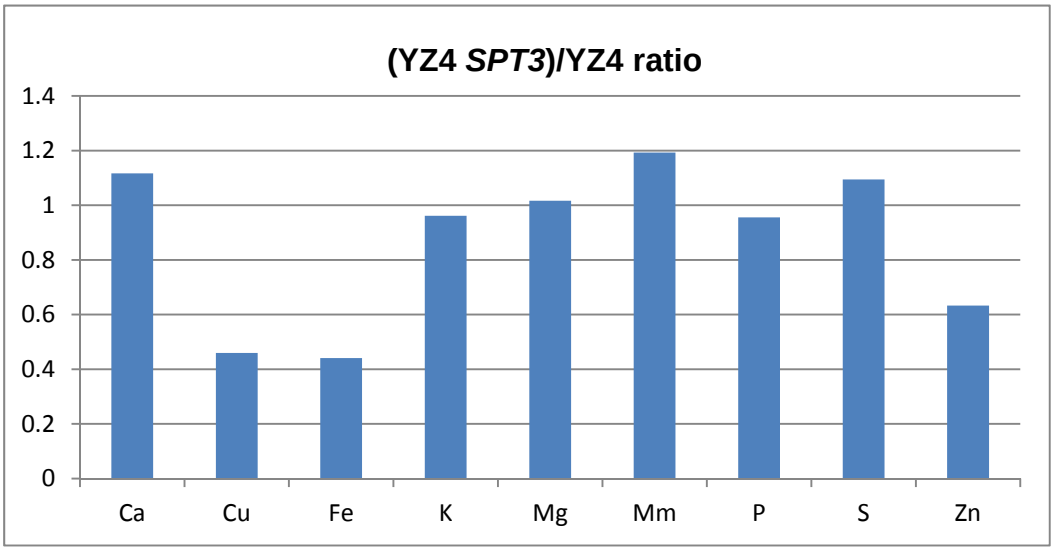

Figure 4.7. The resistant to HU in *aft1⊿aft2⊿* background needs iron, but the iron concentration in YZ4 decreased after rescued by *SPT3*.

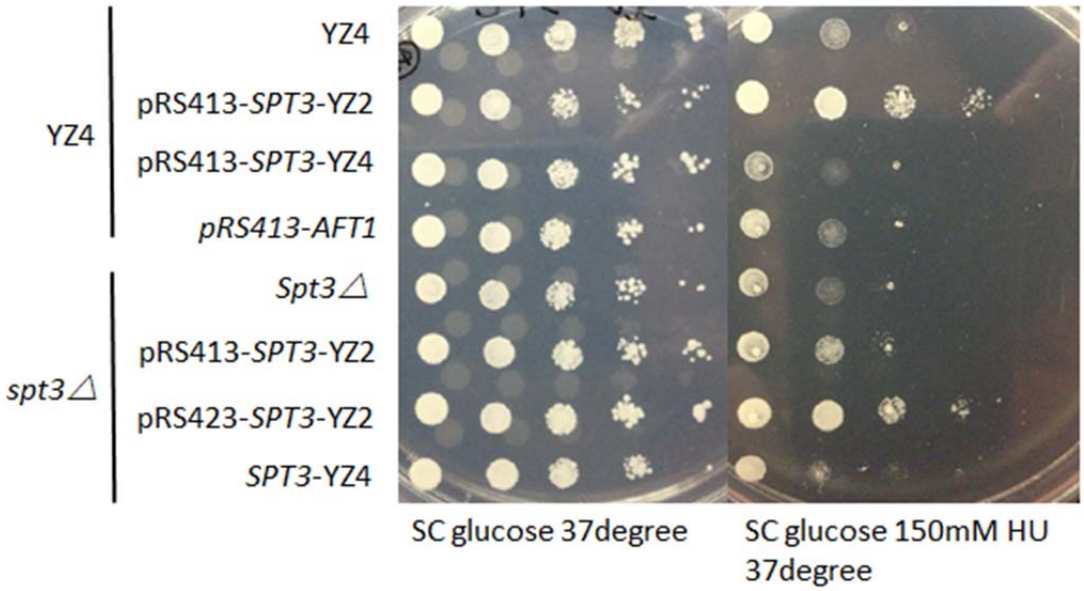

Figure 4.8. Growth test of the HU suppression of YZ4 and BY4741 *spt3⊿*;

BY4741 spt3Δ is HU sensitive phenotype and can be suppressed by *SPT3*.

5. Discussion

Iron transport and delivery in the cytosol must be carefully regulated to limit the potential toxicity of iron while ensuring the delivery to specific targets. In this study we attempted to identify proteins involved in the pathway but isolating suppressors of a hydroxyurea sensitivity in Fe-deficient mutants. Hydroxyurea sensitivity is a result of inhibition of ribonucleotide reductases (RNR) a Fe-containing enzyme required for DNA replication. However the resulting analysis revealed an unknown HU sensitivity gene SPT3.

SPT3 encodes a subunit of the SAGA transcriptional regulation complex and interacts with other members to mediate transcription of RNA-pol II dependent genes. However it can also act as a repressor at certain promoters. Finally it can be inactivated by cytosolic translocation during hypoxia. A survey of SPT3 regulated genes did not reveal obvious reason for the increase in Fe in YZ4 or for the sensitivity to HU. But SPT3 does control PHO84 a gene involved in phosphate metabolism known to affect intracellular metals. Therefore this may be a candidate to affect both Fe and nucleotide production. It should also be noted the SPT3 has 668 known genetic and protein interaction with 375 individual genes so many possible interaction exist.

The original aim attempted to isolate the suppressing mutation from YZ2 but the flawed strategy prevented that mutant being isolated. The YZ4 ability to grow even in the absence of *aft1*Δ*aft2*Δ suggests it also still has a suppressor

mutation. To identify the suppression of the *aft1*Δ*aft2*Δ will need to be repeated in a new background free of additional mutations.

6. Reference

[1] H. Eklund, U. Uhlin, M. Färnegårdh, D. T. Logan, and P. Nordlund, “Structure and function of the radical enzyme ribonucleotide reductase.,” *Prog. Biophys. Mol. Biol.*, vol. 77, no. 3, pp. 177–268, Nov. 2001.

[2] N. T. V Le and D. R. Richardson, “The role of iron in cell cycle progression and the proliferation of neoplastic cells.,” *Biochim. Biophys. Acta*, vol. 1603, no. 1, pp. 31–46, Oct. 2002.

[3] T. Furukawa, Y. Naitoh, H. Kohno, R. Tokunaga, and S. Taketani, “Iron deprivation decreases ribonucleotide reductase activity and DNA synthesis.,” *Life Sci.*, vol. 50, no. 26, pp. 2059–65, Jan. 1992.

[4] J. L. Sneeden and L. A. Loeb, “Mutations in the R2 subunit of ribonucleotide reductase that confer resistance to hydroxyurea.,” *J. Biol. Chem.*, vol. 279, no. 39, pp. 40723–8, Sep. 2004.

[5] A. J. Osborn, S. J. Elledge, and L. Zou, “Checking on the fork: the DNA-replication stress-response pathway.,” *Trends Cell Biol.*, vol. 12, no. 11, pp. 509–16, Nov. 2002.

[6] A. B. Parsons, R. L. Brost, H. Ding, Z. Li, C. Zhang, B. Sheikh, G. W. Brown, P. M. Kane, T. R. Hughes, and C. Boone, “Integration of chemical-genetic and genetic interaction data links bioactive compounds to cellular target pathways.,” *Nat. Biotechnol.*, vol. 22, no. 1, pp. 62–9, Jan. 2004.

[7] C. Dubacq, A. Chevalier, and C. Mann, “The protein kinase Snf1 is required for tolerance to the ribonucleotide reductase inhibitor hydroxyurea.,” *Mol. Cell. Biol.*, vol. 24, no. 6, pp. 2560–72, Mar. 2004.

[8] C. Dubacq, A. Chevalier, R. Courbeyrette, C. Petat, X. Gidrol, and C. Mann, “Role of the iron mobilization and oxidative stress regulons in the genomic response of yeast to hydroxyurea.,” *Mol. Genet. Genomics*, vol. 275, no. 2, pp. 114–24, Feb. 2006.

[9] F. Rodrigues, A. M. Zeeman, C. Alves, M. J. Sousa, H. Y. Steensma, M. Côrte-Real, and C. Leão, “Construction of a genomic library of the food spoilage yeast Zygosaccharomyces bailii and isolation of the beta-isopropylmalate dehydrogenase gene (ZbLEU2).,” *FEMS Yeast Res.*, vol. 1, no. 1, pp. 67–71, Apr. 2001.